

# **Tropical Cyclone Intensity Prediction Using Artificial Intelligence**

**Hamsaa Sayekrishnan**



Department of Earth and Atmospheric Sciences  
**National Institute of Technology Rourkela**

# **Tropical Cyclone Intensity Prediction Using Artificial Intelligence**

*Dissertation submitted in partial fulfillment of*

*the requirements for the degree of*

***Master of Science***

*in*

***Atmospheric Sciences***

*by*

***Hamsaa Sayekrishnan***

(Roll Number: 420AS2144)

*based on research carried out*

*under the supervision of*

***Dr. Krishna Kishore Osuri***



May, 2022

Department of Earth and Atmospheric Sciences  
**National Institute of Technology Rourkela**



Department of Earth and Atmospheric Sciences  
**National Institute of Technology Rourkela**

---

**Dr. Krishna Kishore Osuri**

Assistant Professor

May 13, 2022

## **Supervisors' Certificate**

This is to certify that the work presented in the dissertation entitled *Tropical Cyclone Intensity Prediction using Artificial Intelligence* submitted by *Hamsaa Sayekrishnan*, Roll Number 420AS2144, is a record of original research carried out by her under our supervision and guidance in partial fulfillment of the requirements of the degree of *Master of Science in Atmospheric Sciences*. Neither this dissertation nor any part of it has been submitted earlier for any degree or diploma to any institute or university in India or abroad.

---

Dr. Krishna Kishore Osuri

# Declaration of Originality

I, *Hamsaa Sayekrishnan*, Roll Number 420AS2144 hereby declare that this dissertation entitled *Tropical Cyclone Intensity Prediction using Artificial Intelligence* presents my original work carried out as a Master's student of NIT Rourkela and, to the best of my knowledge, contains no material previously published or written by another person, nor any material presented by me for the award of any degree or diploma of NIT Rourkela or any other institution. Any contribution made to this research by others, with whom I have worked at NIT Rourkela or elsewhere, is explicitly acknowledged in the dissertation. Works of other authors cited in this dissertation have been duly acknowledged under the sections "Reference" or "Bibliography". I have also submitted my original research records to the scrutiny committee for evaluation of my dissertation. I am fully aware that in case of any non-compliance detected in the future, the Senate of NIT Rourkela may withdraw the degree awarded to me on the basis of the present dissertation.



May 13, 2022  
NIT Rourkela

*Hamsaa Sayekrishnan*

# Acknowledgment

I would like to express my sincere gratitude and regard to my project supervisor, Dr. Krishna Kishore Osuri, for the continuous support, advice, and guidance throughout this research project. Without his invaluable time, guidance and encouragement the task would not be completed. The vast knowledge and extraordinary guidance of my supervisor helped me a lot in each and every phase of my research work. I am overwhelmed and feel felicitous for all your support and enthusiasm towards my research work.

No words would sufficiently express my sincere gratitude to my professors Dr. Jagabandhu Panda, Dr. Naresh Krishna Vissa, Dr. Bhishma Tyagi, and Dr. Nagaraju Chilukoti for their constant encouragement and moral support. This project would not have been successful without the knowledge I gained in their practical as well as theory classes. I am also thankful to Dr. Bhaskar Kundu, Dr. Md. Equeenuddin, Dr. Rekha S., and Dr. Thungyani N. Ovung for their valuable support and encouragement.

I also take the opportunity to express my sincere thanks to Sasanka Talukdar (Junior Research Fellow) and Buri Vinodh Kumar, Nekkali Yerni Srinivas, Priya Kumari, Tirumani Siva Sai Krishna (Ph.D. Scholars) of our lab for their constant support and encouragement to complete this task.

I owe special thanks to my friends for their encouragement and moral support to complete this project. Last, but not least, I would like to express a heartfelt thanks to my family members for their unconditional support and encouragement while carrying out the research work.



May 13,2022  
NIT Rourkela

*Hamsaa Sayekrishnan*  
Roll Number: 420AS2144

# Abstract

Accurate forecasting of TC intensity and trajectory is becoming an increasingly important part of catastrophe preparedness and response. Deep learning approaches outperform dynamical and statistical models in capturing the complicated nonlinear connection of TC intensity fluctuations. In this study, the single-step prediction of the Intensity of tropical cyclones is done using AI models for the North Indian Ocean basin based on large-scale environmental features. The climatology plots and Pearson's correlation for the various features were used to extract 10 features correlated with TC intensification. Comparing the Support Vector Machine (SVM) regressor, Random Forest (RF) Regressor, and Long Short Term Memory (LSTM) model for the India Meteorological Department (IMD) and Joint Typhoon Warning Centre (JTWC) data-frame, LSTM performed the best with the highest correlation and least error (Bias/ RMSE) for 12hr to 24hr forecasts. TC intensity is accurately predicted, with a mean bias of -3 m/s for 12 hr forecast and 6.6m/s for 24hr forecast. Upon comparing the IMD and JTWC datasets based on the density of the bias distribution, IMD is more accurate as the maximum density of bias is located around 0 when compared to JTWC. The strong correlation value with a constant bias indicates that the bias correction can be performed for better forecast accuracy.

**Keywords:** *Tropical Cyclone; Intensity Prediction; Artificial Intelligence*

# Contents

<b>Supervisor's Certificate</b>	<b>i</b>
<b>Declaration of Originality</b>	<b>ii</b>
<b>Acknowledgement</b>	<b>iii</b>
<b>Abstract</b>	<b>iv</b>
<b>Contents</b>	<b>v</b>
<b>List of Figures</b>	<b>vi</b>
<b>List of Tables</b>	<b>viii</b>
<b>Chapter 1 Introduction</b>	<b>1-5</b>
1.1 Background and Purpose	1
1.2 Literature review	2
1.3 Research Gaps	4
1.4 Significance and Objective	5
<b>Chapter 2 Data and Methodology</b>	<b>6-12</b>
2.1 Data	6
2.2 Methodology	7
2.3 Machine Learning and Deep Learning Models	8
<b>Chapter 3 Results and Discussion:</b>	<b>13-45</b>
3.1 Feature Extraction	13
3.2 Prediction Using Machine Learning	27
3.3 Prediction Using Deep Learning	32
<b>Chapter 4 Conclusions and future scopes</b>	<b>46- 47</b>
<b>References</b>	<b>48</b>

## List of Figures

<b>Fig No.</b>	<b>Caption</b>	<b>Page No.</b>
1	Flowchart describing the methodology	8
2	Random Forest regressor Architecture	10
3	LSTM cell	11
4	MSLP from JTWC and IMD extracted centres	13
5	Vorticity from JTWC and IMD extracted centres	14
6	Total precipitation from JTWC and IMD extracted centres	15
7	Mean wind shear between 850hPa and 200hPa from JTWC and IMD extracted centres	16
8	Mean wind at 850hPa from JTWC and IMD extracted centres	17
9	Mean wind at 200hPa from JTWC and IMD extracted centres	18
10	Specific Humidity at 700hPa from JTWC and IMD extracted centres	19
11	Specific Humidity at 750hPa from JTWC and IMD extracted centres	20
12	Specific Humidity at 800hPa from JTWC and IMD extracted centres	21
13	Specific Humidity at 850hPa from JTWC and IMD extracted centres	22
14	Excluded features: CAPE, Upper-level Divergence and SST anomalies	23
15	Correlation Heatmap of JTWC with respect to Vmax	25
16	Correlation Heatmap of IMD with respect to Vmax	26
17	JTWC Random Forest (RF) test data forecasts	27
18	IMD RF test data forecasts	28
19	JTWC Support Vector Machine (SVM) test data forecasts	29
20	IMD SVR test data forecasts	30
21	LSTM train and test loss curves for the JTWC dataset	32
22	LSTM train and test loss curves for IMD dataset	33
23	LSTM actual and predicted Vmax for the JTWC dataset	35

24	LSTM actual and predicted Vmax for IMD dataset	36
25	Comparison of the distribution of bias between actual and predicted Vmax	37
26	Bias Box plot for JTWC validation dataset for each cyclone	38
27	Bias Box plot for IMD validation dataset for each cyclone	38
28	Scatter plots between actual and forecast Vmax for JTWC dataset	41
29	Scatter plots between actual and forecast Vmax for IMD dataset	42
30	Correlation between actual and forecast Vmax for IMD and JTWC datasets	42
31	Bias between actual and forecast Vmax for IMD and JTWC datasets	43
32	RMSE between actual and forecast Vmax for IMD and JTWC datasets	43

## List of Tables

<b>Table No.</b>	<b>Caption</b>	<b>Page No.</b>
1	Classification of TC in NIO as per IMD guidelines	2
2	List of features Considered	6
3	Pearson's correlation Values	24
4	JTWC error metrics for RF	27
5	IMD error metrics for RF	28
6	JTWC error metrics for SVM	29
7	IMD error metrics for SVM	30
8	LSTM model summary	31
9	Validation data: 2017 - 2019 for both IMD and JTWC datasets	33
10	Error statistics against IMD trained model	39
11	Error statistics against JTWC trained model	40
12	Error Statistics summary for intensity prediction (Vmax) for IMD and JTWC trained model	44

# **Chapter 1**

## **Introduction**

### **1.1 Background and purpose**

Tropical cyclones (TCs) are low-pressure systems that form over warm tropical oceans. They are catastrophic natural disasters that affect many countries and cause loss of lives and property destruction. The tropical cyclones work as heat engines. They draw energy from the ocean for their formation. These cyclonic systems rotate counter-clockwise in the northern hemisphere, while in the southern hemisphere, they rotate in the clockwise direction. TCs have different names in different regions. They are also known as Hurricanes in the North Atlantic and the eastern North Pacific oceans, typhoons in the western North Pacific Ocean and tropical cyclones over the Indian Ocean and South Pacific.

The favourable environmental conditions important for tropical cyclogenesis over an ocean basin are as follows:

- I. Large values of low-level relative vorticity, i.e., a vortex, should be prevalent
- II. The cyclonic system should form approximately 50° away from the equator i.e., Coriolis force should be strong and sufficient enough to produce a rotational effect and help in maintaining the low pressure of the disturbance.
- III. Weak vertical wind shear, i.e., less than  $10 \text{ ms}^{-1}$  (wind shear in North-South direction do not significantly impact the storms (Gray 1968)).
- IV. High SST and deep thermocline (i.e.,  $\text{SST} > 26.5^\circ\text{C}$  and temperature should be high enough up to a sufficient depth of about 50-60 m).
- V. Conditional instability through a deep atmospheric layer
- VI. Large values of relative humidity in the middle and lower troposphere

The average annual frequency of tropical cyclones in the North Indian Ocean (the Bay of Bengal (BoB) and the Arabian Sea (AS)) is about 5-6 % of the global annual average (Dube et al., 1997). Since the AS is relatively cooler, the formation and intensification of tropical cyclones are comparatively lesser than BoB (Kumar et al., 2016). TCs formed over the North

Indian Ocean (NIO) region are classified based on maximum sustained wind speed (MSW) associated with the system as per India Meteorological Department (IMD) guidelines. When the system is over land pressure criteria is used, and wind criteria are used when the system is over the sea. Accordingly, the TCs over the NIO region can be categorized into seven types, as given in Table 1.

**Table1:** Classification of TC in NIO as per IMD guidelines

SYSTEM	WIND SPEED (knots)
Low	<17
Depression	17-27
Deep Depression	28-33
Cyclonic Storm	34-47
Severe Cyclonic Storm	48-63
Very Severe Cyclonic Storm	64-90
Extremely Severe Cyclonic Storm	91-119
Super Cyclonic Storm	>119

## 1.2 Literature Review

Track and intensity forecasts are the two important TC parameters, indicating where the TC will go and how strong the winds will be. In recent times, track prediction has improved significantly, but not the intensity prediction.

Tropical cyclones (TCs), together with gales, rainstorms, and storm surges, are considered catastrophic weather occurrences that can cause massive losses of life and property in coastal areas around the world. As a result, accurate forecasting of TC intensities and trajectories becomes an increasingly important and essential part of catastrophe preparedness and response. The physical mechanisms involved in TC, however, are complex and difficult to accurately

characterise using dynamic equations, making TC prediction problematic. The enormous improvements in trajectory prediction over the last few years have been attributed to advances in dynamical weather prediction models. Unlike TC trajectory prediction, which has improved considerably over time, TC intensity prediction has improved modestly over time and remains a difficult topic to master (Yang et al., 2020).

The limitations of the forecasting process have hampered the advancement of TC intensity prediction. In the TC forecast, dynamical or the statistical forecast models are commonly used, with the dynamical models which are based on a couple of equations based on fluid mechanics and the statistical models examining empirical relationships from historical TC records and related variables using standard statistical methods. Unlike typical meteorological events and oceanic processes, TC dynamics are complicated, and fluctuations in TC intensity are influenced by a variety of nonlinear environmental variables. Unfortunately, dynamical and statistical models are less capable than deep learning methods of capturing the complicated nonlinear relationship between TC intensity variations (Zhang et al., 2022).

The successful implementation of deep learning methods in various fields which are data driven indicated that deep learning methods can efficiently extract spatial and temporal information from multi-source data. As a result, some academics have attempted to investigate the topic of predicting TC intensity using deep learning algorithms.

Feng et al. (2005), used a dynamic neural network classifier which predicts the maximum potential intensity of the cyclone (MPI). They used a 10-year period of tropical cyclones formed over the Western north pacific and the monthly mean sea surface temperature. For fast and accurate neural network training, a strategy to determine the most significant-correlated features of tropical cyclones was developed. The structure of the network layers is adjusted using a binary trigger. To justify the performance, we conduct a series of tests to demonstrate that our proposed model is viable.

Sutap et al. (2012), developed a Multi-Layer Perceptron (MLP) model for TC intensity prediction in the North India Ocean (NIO). This was based on environmental variables such as central pressure, sea surface temperature, maximum sustained surface wind speed, pressure drop and ozone column. The intensity is predicted as per the T - number of the cyclone. The MLP model has been shown to be capable of accurately forecasting the intensity of tropical cyclones with minimal forecast error (4.70%).

Kirkwood et al. (2019), For TC intensity prediction, built a feed-forward neural network (FFNN). This had incorporated both the real-time estimate of current intensity ( maximum 1min averaged 10m wind speed) and predictors obtained from operational model forecasts-Hurricane weather research and forecasting(HWRF) model The neural network outperformed the HWRF in terms of mean absolute error (MAE) at all lead-times, and it was consistently better than the observation-adjusted HWRF as the lead-time increased.

Despite the excellent advancement in the TC intensity prediction task, the MLP's capacity to handle temporal information is limited. Hence, some researchers approached predicting TC intensity as a time series problem involving multiple environmental variables.

Regression Neural Network (RNN) was used to extract temporal relations from huge TC past observation data over the Western North Pacific, since 1949, and built a fully data-driven TC intensity prediction model. In a 24-hour prediction, the proposed method had a 5.1 m/s inaccuracy, which is better than several commonly used dynamical models and near to subjective prediction (Bin Pan et al., 2019).

Shijin Yuan et al. (2021), suggested a TC forecasting model based on the long short-term memory (LSTM) network. To determine the best prediction parameters, the typhoon intensity forecasting models are first trained and evaluated using processed typhoon data from 2000 to 2014. The models are then evaluated against a feed-forward neural network using the best prediction factors (FNN). The model based on LSTM using the optimal prediction factors shows the best performance and lowest prediction errors. As a result, the LSTM-based model is useful for predicting typhoon severity within 120 hours.

A Bi-Directional based LSTM-based Recurrent Neural Network (RNN) model was created over the NIO to predict the landfall intensity based on maximum sustained surface wind speed (MSWS). The model has predicted MSWS (in knots) for the next 3, 12, 24, 36, 48, 60, and 72 hours with a mean absolute error of 3.66, 5.88, 8.96 and 11.92, respectively for 12 hr, 24 hr, 48 hr and 72 hr forecasts (Biswas et al., 2021).

### 1.3 Research Gaps

This study revealed the efficiency of deep learning algorithms in forecasting TC intensity, and two critical parameters for increasing prediction performance were found.

For starters, more TC-related environmental variables should be incorporated. For most short-term disaster forecasting operations, historical disaster data alone has low predictive value. As a result, many environmental variables are included in specific research to improve the prediction accuracy of approaching disasters or climate events. Second, both spatial and temporal parameters must be incorporated to develop a complete TC intensity forecast model.

The deep learning method is thought to be more effective with more environmental variables based on the above methodologies. The quality and number of features retrieved and supplied to the model will aid in the development of a complete model for predicting TC intensity. The fundamental flaws of the methods outlined above are that feature extraction is simply a concatenation, but each variable has a unique connection with TC intensity, which the model must be able to capture for higher accuracy.

#### **1.4 Significance and Objective**

In order to accurately predict the TC intensity, we need to study the large-scale environmental features that affect the tropical cyclone intensity measured using Maximum sustained wind speed. The ability of AI models to outperform dynamical and statistical models along with computational efficiency and due to the lack of extensive work to predict the TC intensity over NIO using AI methods with large-scale environmental features, the following objective is proposed,

*“To predict the Intensity of tropical cyclones using AI models for the North Indian Ocean basin based on large-scale environmental features.”*

## **Chapter 2**

### **Data and Methodology**

#### **2.1 Data**

The Study is confined to the North Indian Ocean which includes the Bay of Bengal and the Arabian Sea. The data used in the study comprises best track data and reanalysis data. The Joint Typhoon Warning Centre (JTWC) Best Track data comprising 5015 samples and Indian Meteorological Department (IMD) Best Track data comprising 6264 samples were used. The time period of the analysis is between 1982-2019. The training period is between 1982-2017 and validation period is between 2017-2019. The ERA5 Reanalysis Data from European Centre for Medium-Range Weather Forecasts (ECMWF) for the Environmental Features with  $0.25^\circ \times 0.25^\circ$  resolution was used for downloading data for large scale environmental features. The environmental features considered are as shown in Table 2. The feature to be predicted is the maximum sustained wind speed (Vmax).

**Table 2:** List of features Considered

S . No.	LARGE SCALE ENVIRONMENTAL FEATURES
1.	Sea Surface Temperature (SST)
2.	Mean Sea Level Pressure (MSLP)
3.	Vorticity at 850hPa
4.	Divergence at 200hPa
5.	Total Precipitation
6.	Specific Humidity at 700hPa
7.	Specific Humidity at 750hPa
8.	Specific Humidity at 800hPa
9.	Specific Humidity at 850hPa

10.	Mean Wind at 850hPa
11.	Mean Wind at 200hPa
12.	Mean Wind shear between 850hPa and 200hPa
13.	Convective Available Potential energy (CAPE)

### 2.3 Methodology

ERA5 TC centres were extracted using the best track data centres based on Minimum Mean Sea level pressure criteria within a 500 km radius. Based on the extracted centres, the reanalysis data for the environmental features were converted to polar coordinates and rotated to align the direction of movement of TCs to the North. Using the converted data, the climatology of the features and Pearson's correlation were calculated between the features and the maximum sustained surface wind speed (Vmax) to extract the features with maximum correlation. The features were averaged over a radius of 500 km, and the averaged value was used to represent the feature at a particular centre. The data frame hence prepared from JTWC and IMD best track data is then used to run Machine Learning models like Random Forest Regressor (RF) and Support Vector Machine Regression (SVM) and Deep Learning models such as Long short-term memory (LSTM). Intensity forecasting was done on the data from 6 hr to 72 hr time steps (Fig 1).

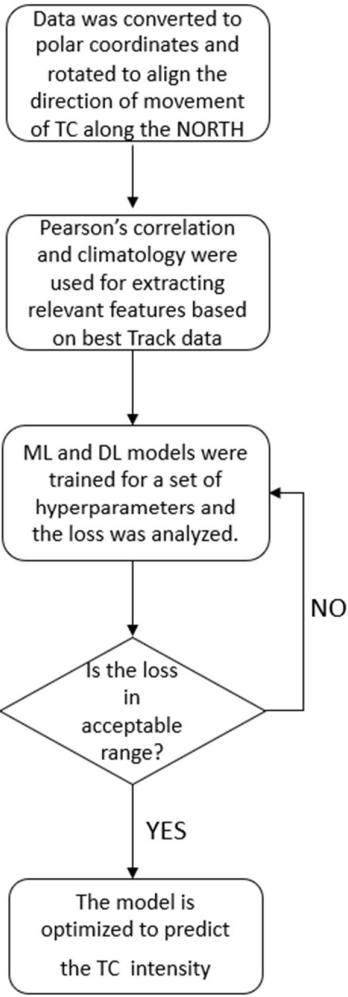


**Fig 1:** Flowchart describing the methodology

## 2.3 Machine Learning and Deep Learning Models

### 2.3.1 Support Vector Machine (SVM)

Machine learning tool SVM is a supervised statistical learning algorithm for Classification and Regression. SVM is an algorithm for maximising a particular mathematical function with respect to a given data. SVM can be summarised based on four concepts, the separating hyperplane, the maximum margin hyperplane, the soft margin, and the kernel function. The separating hyperplane is a straight line in higher dimensional space, used to separate various groups of samples. The maximum margin hyperplane can be defined with the following statement. The SVM selects the maximum margin separating hyperplane if the distance

between the separating hyperplane and the nearest expression vector is defined as the margin of the hyperplane. Soft margin allows data to find its way through the margin of the separating hyperplane without affecting the final output. Finally, the kernel function projects data from a lower-dimensional space to a higher-dimensional space.

The training instances are used to separate classes by the separating hyperplane, the maximum separation from the classes is located by the maximum margin hyperplane and it is an optimal hyperplane, the soft margin allows some of the imperfect instances to be misclassified so the result will be unaffected, the kernel function is used for mapping of input shape to the feature shape and decreasing the computational efforts.

SVM constructs an  $n-1$  dimensional plane for  $n$  dimension space with features of SVM classes. This hyperplane was selected as it has a maximum distance for classes. It called as maximum margin hyperplane and the separating hyperplane equation express as –

$$w \cdot x + b = 0$$

x: D-dimensional feature matrix consisting features of input classes

b: Bias

w: Normal to the hyperplane (weights)

For the real word problem, it is hard to perfectly separate these classes so the soft margin allows some misclassified instances with some limits, the input space is mapped into feature space using kernel function, the hyperplane equation-

$$f(x) = \text{sgn}(q(x) \cdot w + b) \quad (\text{Noble, 2006})$$

### 2.3.2 Random Forest regressor

A random forest is a supervised learning algorithm that uses ensemble learning of decision trees for regression. The tree-based models involve partitioning the dataset into two groups based on criteria until the stopping condition is met. Depending on the criteria, the decision trees can be used for classification and regression tasks.

The process can be understood as,

- Pick a random k data point from the training set
- Build a decision tree associated with these k data points
- Choose the number N of trees you want to build and repeat.
- For the new data point, make each one of your N tree trees predict the value of y for the data point in question and assign the new data point to the average across all of the predicted y values (Schonlau et al., 2020).

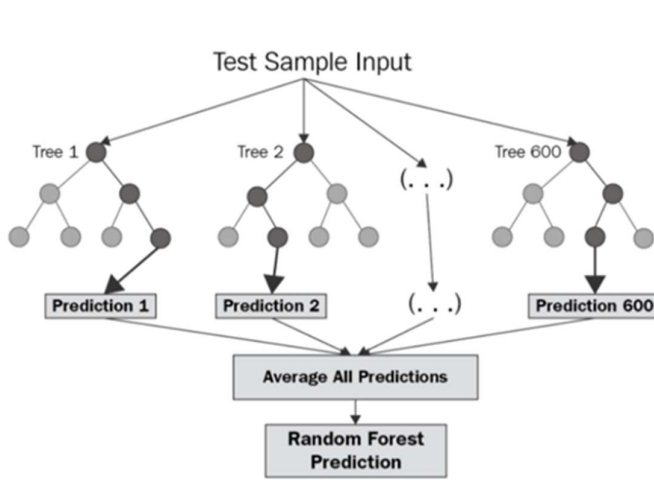


**Fig 2:** Random Forest Regressor Architecture

### 2.3.3 Long Short-Term Memory (LSTM)

LSTM is a special kind of Recurrent Neural network (RNNs) that are capable of learning dependencies for long terms by remembering the pattern. LSTM is special because of its memory blocks. It has a combination of networks in loops, where it contains different types of activation function layers and gates for their specific role.

The current state is split into two vectors - short term state  $\mathbf{h}_{(t)}$  and long term state  $\mathbf{c}_{(t)}$ . The current input vector  $\mathbf{x}_{(t)}$  and the previous short term state  $\mathbf{h}_{(t-1)}$  are fed to four different fully connected layers. The main layer outputs  $\mathbf{g}_{(t)}$  by analysing the current input and the previous state. The most important parts of this layer are stored in an output state. The three other layers are gate controllers (output range from 0 to 1). The forget gate  $\mathbf{f}_{(t)}$  controls which part of long term state must be erased. The input gate  $\mathbf{i}_{(t)}$  controls which parts of  $\mathbf{g}_{(t)}$  should be added to the

long term state. The output gate  $\mathbf{o}_{(t)}$  controls which parts of the long term state should be read and output at this time step.

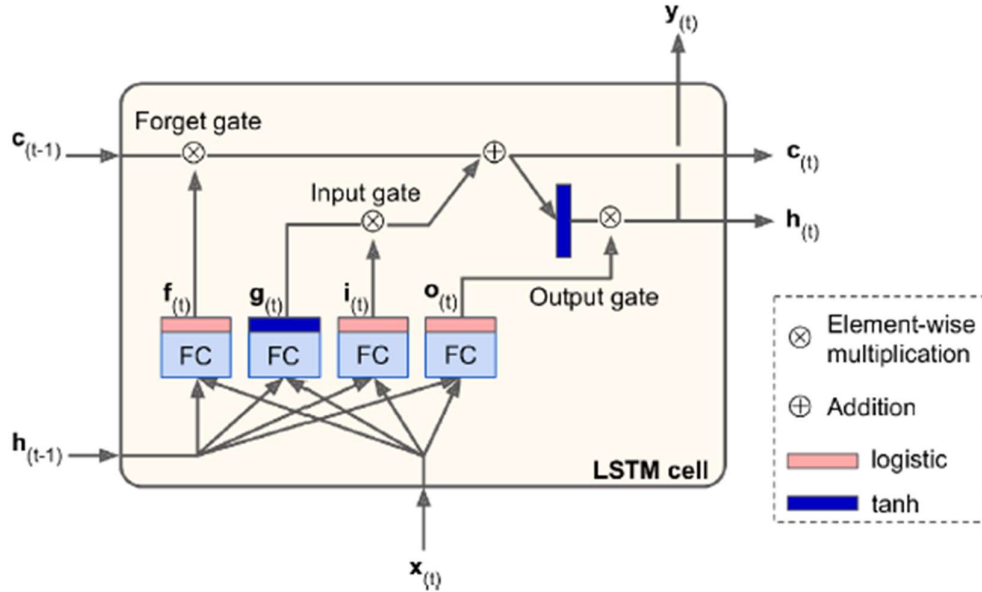


**Fig 3:** LSTM cell

LSTM can be understood by the following steps-

**Step 1.** By using the Sigmoid layer this forget gate ( $f_t$ ) decide which memory will be stored and which will be thrown away, the function for this forget gate can be understood by this equation,

$$f_t = \sigma(W_{sf}^T \cdot X_t + W_{hf}^T \cdot h_{(t-1)} + b_f)$$

$\sigma$  – sigmoid activation function

$X_t$  – input

$h_{(t-1)}$  – previous hidden state

The output lies down between zero to one and for every number in the cell state  $Ct-1$ , zero represents ‘get rid of it completely’ and one represents ‘keep this completely’

**Step 2.** The decision for storing new information in cell state is decided by both Input gate ( $i_t$ ) and candidate cell  $g_{(t)}$ . The function can be defined by the equation,

$$i_t = \sigma(W_i \cdot X_t + W_i \cdot h_{(t-1)} + b_i)$$

$$g_t = \tanh(W_{ng}^T \cdot X_t + W_{hg}^T \cdot h_{(t-1)} + b_g)$$

$W_i, b_i, W_{hg}, b_g$  – weight and bias of  $i_t, g_t$

The output value for the tanh activation function is between -1 to 1. The following equation expresses how the combination of  $i_t, C_{t-1}$  and  $g_t$  create a new update for the state,

$$C_t = f_t \cdot C_{t-1} + i_t \cdot g_t$$

And the old information is dropped out by the network and  $c$  is considered as a new cell state.

**Step 3.** The output information from the memory is control by the Output gate ( $o_t$ ), and the function can be express by the following equations,

$$o_t = \sigma(W_{xo}^T \cdot X_t + W_{ho}^T \cdot h_{(t-1)} + b_o)$$

$$y_t = o_t \cdot \tanh(c_t)$$

$W_f, b_f, W_c, b_c$  – weight and bias of  $f_t$

and new cell state and hidden state.

The advantage of the neural network over regression-based is that in regression we assume the function first like linear or exponential then we perform iteration to reduce the error but in a neural network, the method itself extracts the function from the data provided. The most commonly used network is a feed-forward neural network. It consists of a set of nodes interlinked with each other and each node contains a neuron that performs a computational function. The network is arranged one after another such that the output of one node is input for another node.

# Chapter 3 Results and Discussion

## 3.1 Feature Extraction

### 3.1.1 Climatology of the features

In Order to gain more insights from the data, the climatology of the environmental features was plotted to detect the spatial patterns. Deep learning algorithms can easily detect patterns and formulate a relationship based on it with the variable to be predicted.

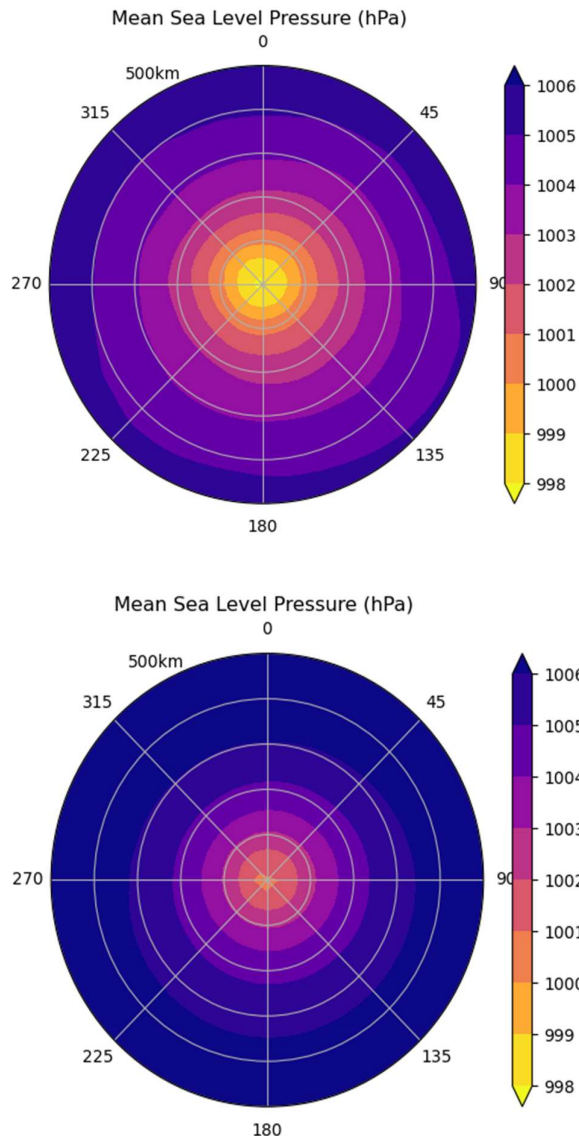


**Fig 4:** MSLP from JTWC centres (up) and MSLP from IMD extracted centres (below)

The MSLP is minimum at the eye of the cyclone and increases with radius. As shown in the diagram above, using both datasets, the spatial patterns match each other and are consistent with the literature review. The minimum pressure is around 998hPa and the maximum is around 1006hPa (Fig 4).

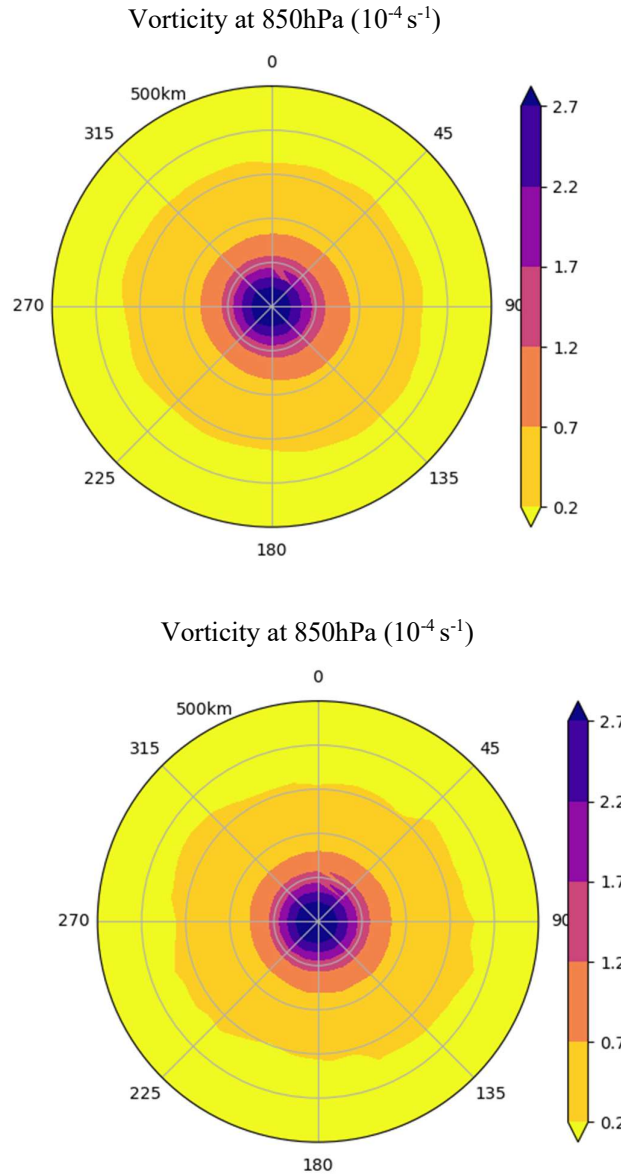


**Fig 5:** Vorticity from JTWC centres (up) and Vorticity from IMD extracted centres (below)

The vorticity at 850hPa or the lower-level vorticity indicates the convergence or the inflow at the lower level (850hPa). The convergence is highest at the centre and decreases with radius,

due to the Minimum Sea level pressure at the centre. Larger the vorticity, the easier it is for the storm to organise itself (Fig 5). The total precipitation within a radius of 500 km from the centre of the TC is found to be maximum around the eyewall region (Vinodhkumar et al.,2020). The climatology plots of Total precipitation indicate a similar pattern, with maximum precipitation of 4 mm around the centre and a minimum of 0mm (Fig 6).

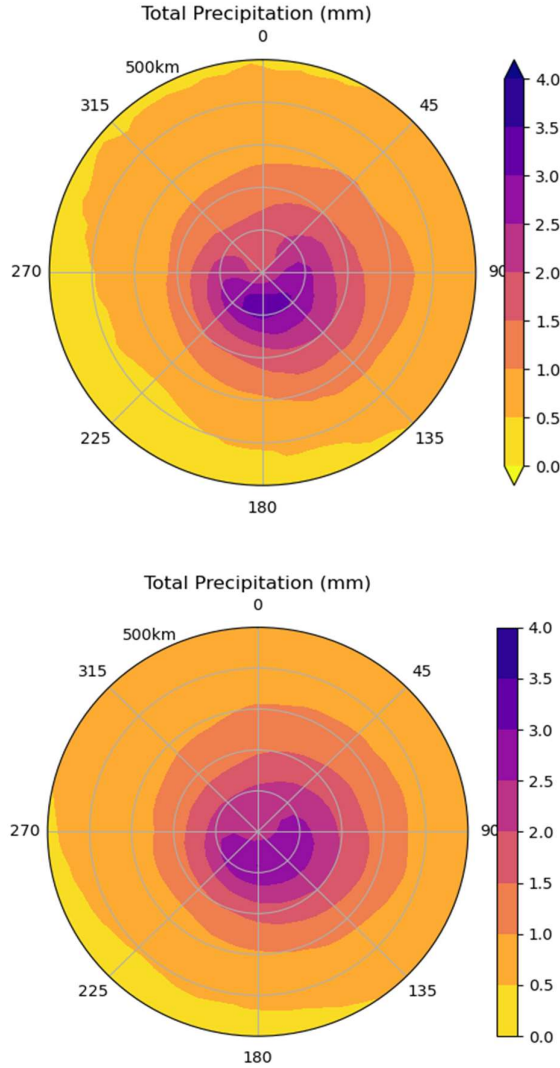


**Fig 6:** Total Precipitation from JTWC centres (up) and Total Precipitation from IMD extracted centres (below)

The mean wind shear between 850hPa and 200hPa is the difference between the winds at 850hPa and 200hPa. For a TC to intensify the wind shear must be weak, as stronger the shear, If the shear is too strong, the updrafts in the thunderstorms become tilted, and latent heating

due to water-vapour condensation is spread over a broader area. This results in less-concentrated warming, and a reduced ability to create a low-pressure centre at sea level around which the thunderstorms can become organized into a hurricane (Fig7).

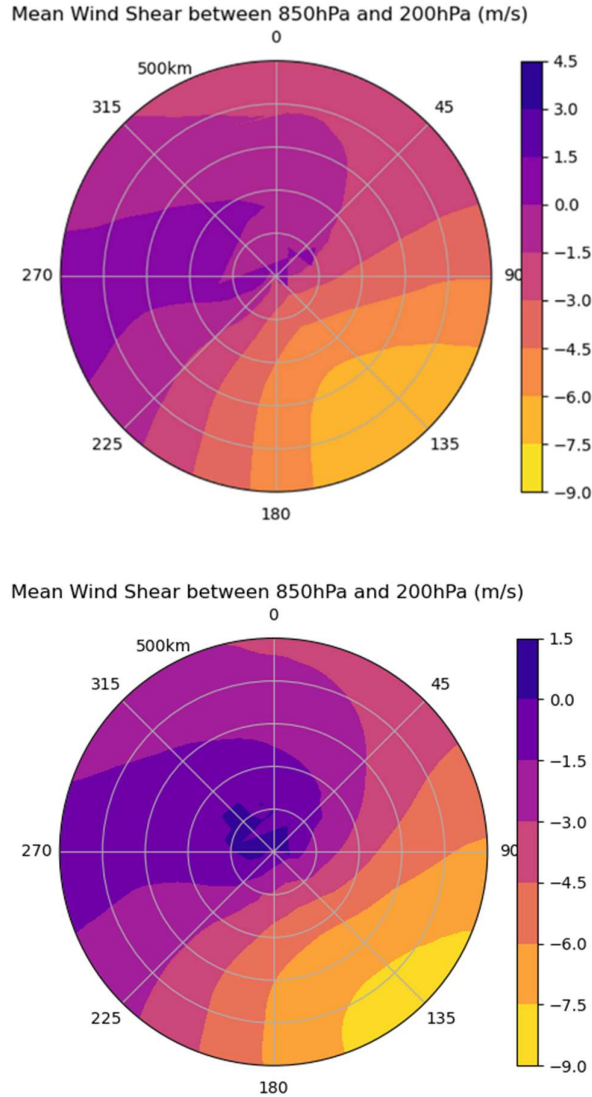


**Fig 7:** Mean wind shear between 850hPa and 200hPa from JTWC centres (up) and from IMD extracted centres (below)

The mean wind at lower and upper levels (850hPa and 200hPa respectively) are shown below (Fig 8 and 9). The mean wind at 850hPa is maximum at the forward sector of the TC. The maximum mean wind at lower levels is around 13m/s and the minimum mean wind is around 5-7 m/s. The upper-level winds must also be high due to divergence aloft. Stronger the winds

indicate more divergence. The maximum upper-level wind is around 15m/s and the minimum upper-level wind is around 10m/s.

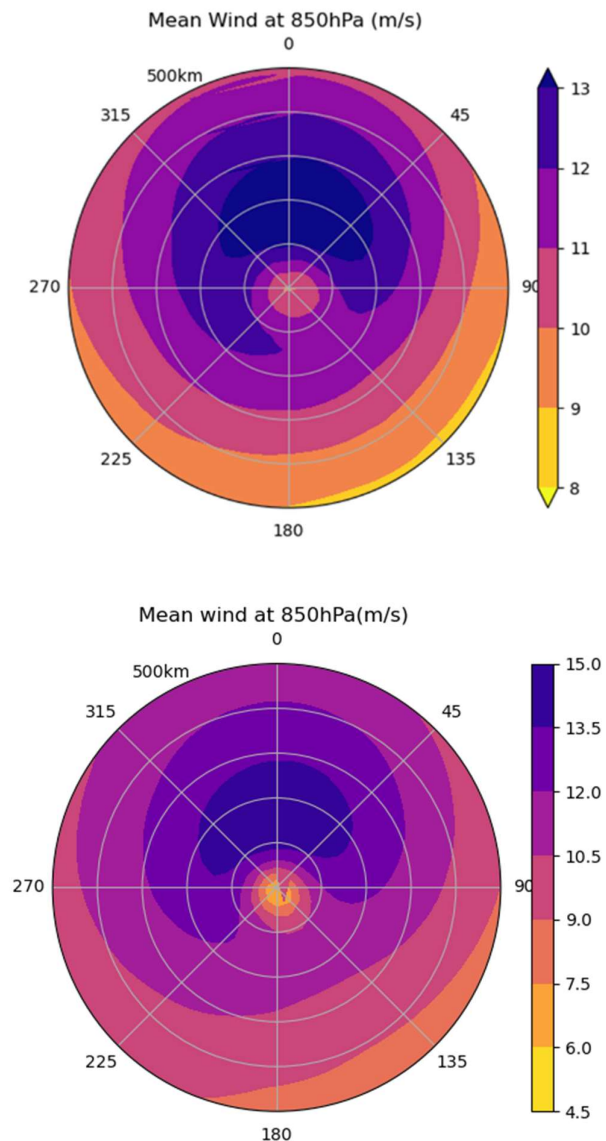


**Fig 8:** Mean wind at 850hPa from JTWC centres (up) and from IMD extracted centres (below)

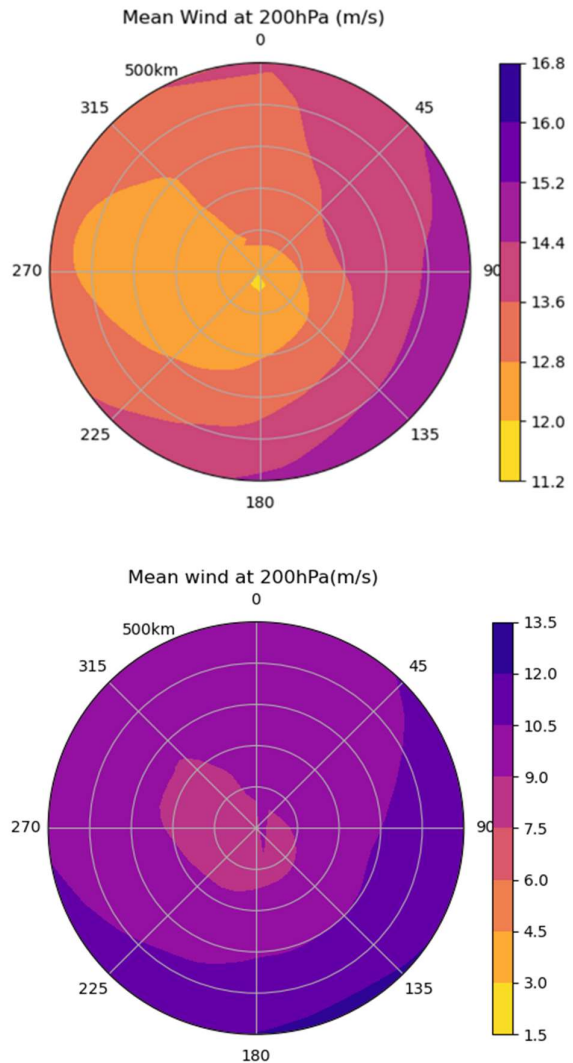


**Fig 9:** Mean wind at 200hPa from JTWC centres (up) and from IMD extracted centres (below)

The specific Humidity between 850hPa and 700hPa is shown in the below figures (Fig 10,11,12,13). High mid-tropospheric humidity is essential, otherwise, the thunderstorms cannot grow into TCs. Note that this differs from mid-latitude thunderstorms, where a drier mid-troposphere allows more violent thunderstorms.

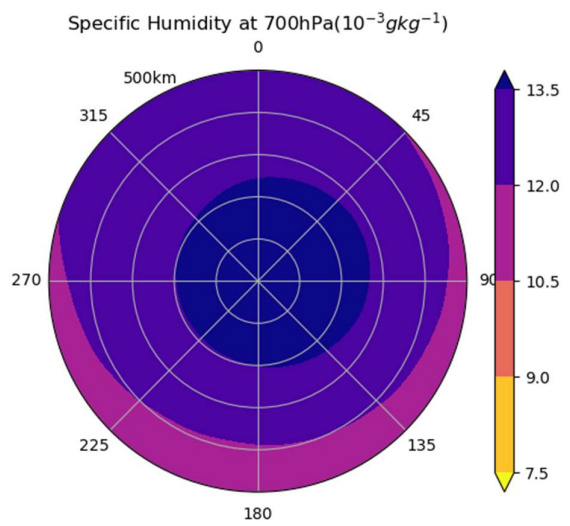
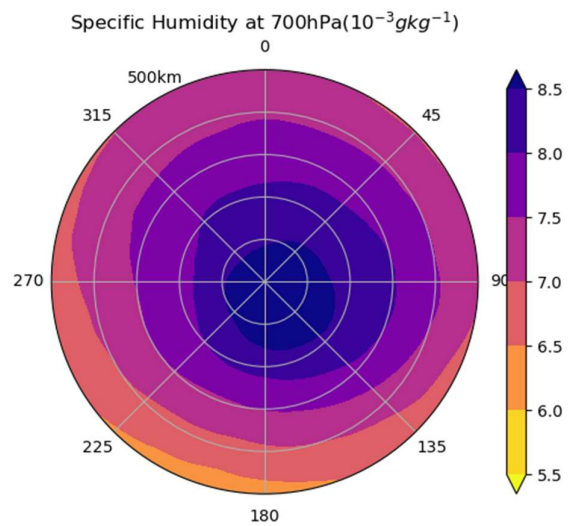


**Fig 10:** Specific Humidity at 700hPa from JTWC centres (up) and from IMD extracted centres (below)

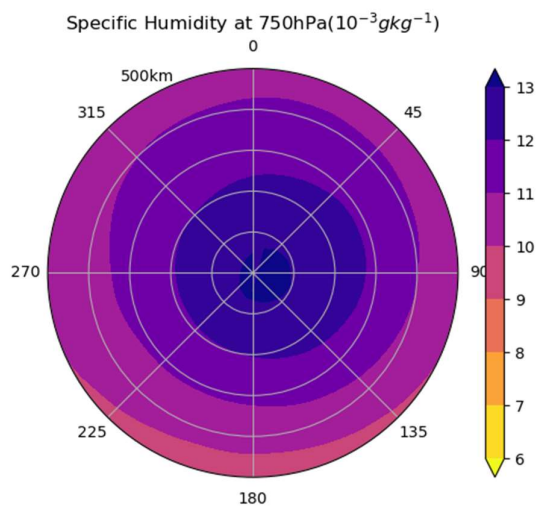
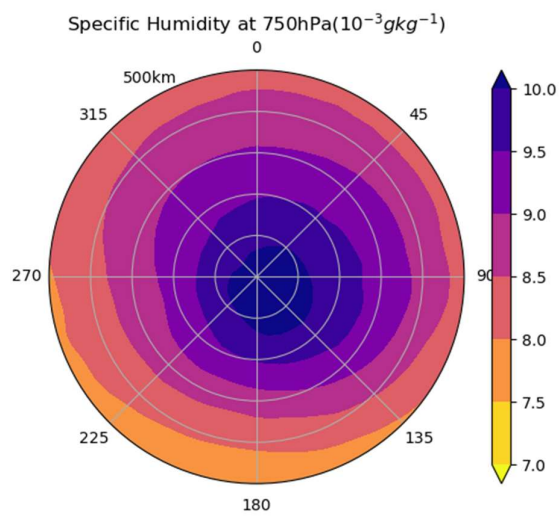


**Fig 11:** Specific Humidity at 750hPa from JTWC centres (up) and from IMD extracted centres (below)

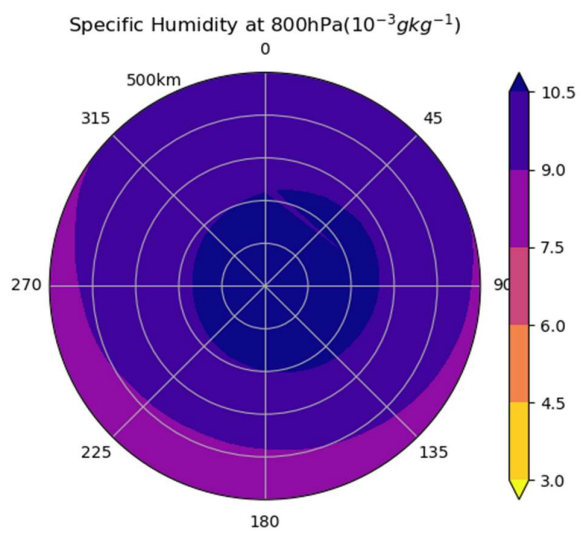
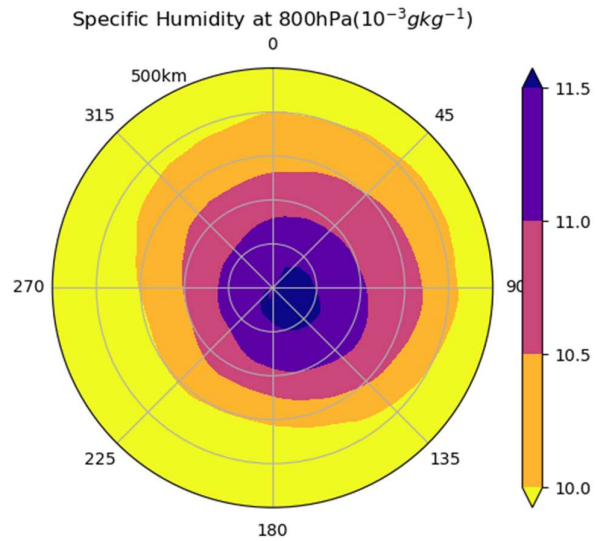


**Fig 12:** Specific Humidity at 800hPa from JTWC centres (up) and from IMD extracted centres (below)

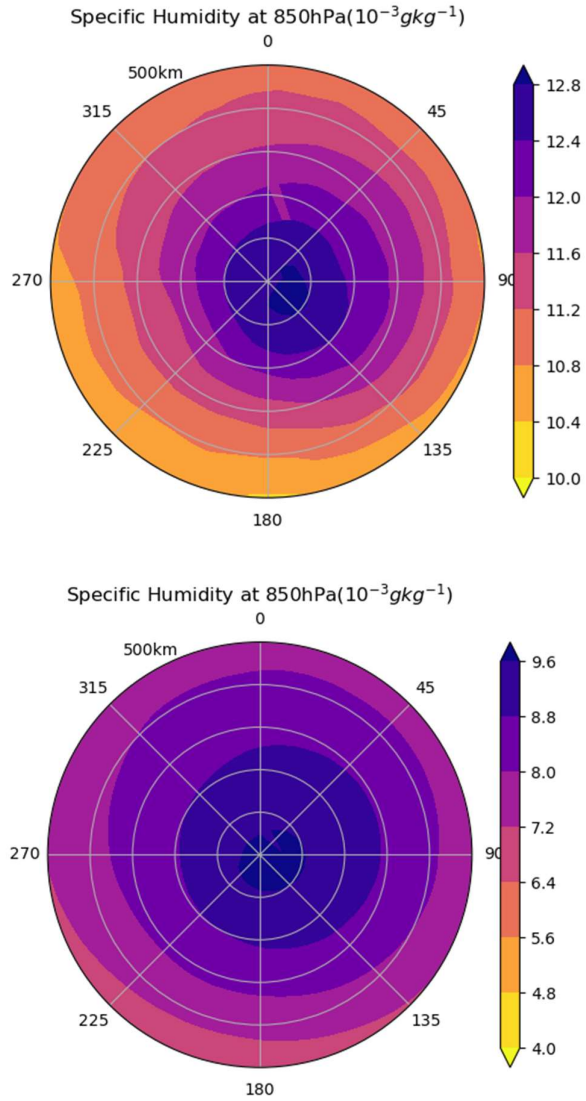


**Fig 13:** Specific Humidity at 850hPa from JTWC centres (up) and from IMD extracted centres (below)

The Upper-level Divergence and Sea Surface temperature were excluded from the features due to their low correlation and lack of spatial pattern, inconsistent with the literature. The SST anomalies shown below indicate the warm region left of the cyclone and the cold region right of the cyclone. But according to literature, the warm region is ahead of the cyclone and the cold region is behind the cyclone, due to the cooling initiated. The upper-level divergence is highly correlated with Lower-level vorticity and upper-level mean winds and hence the removal of the feature would not lead to loss of data for the model. The Convective available potential energy for a TC must be maximum at the centre region of the storm as that indicates maximum instability. But the CAPE is found to be minimum with 400 J/kg of energy at the centre and

increases with radius, thus inconsistent with the literature and hence is excluded from the features. The plots of the excluded features are shown below (Fig14).

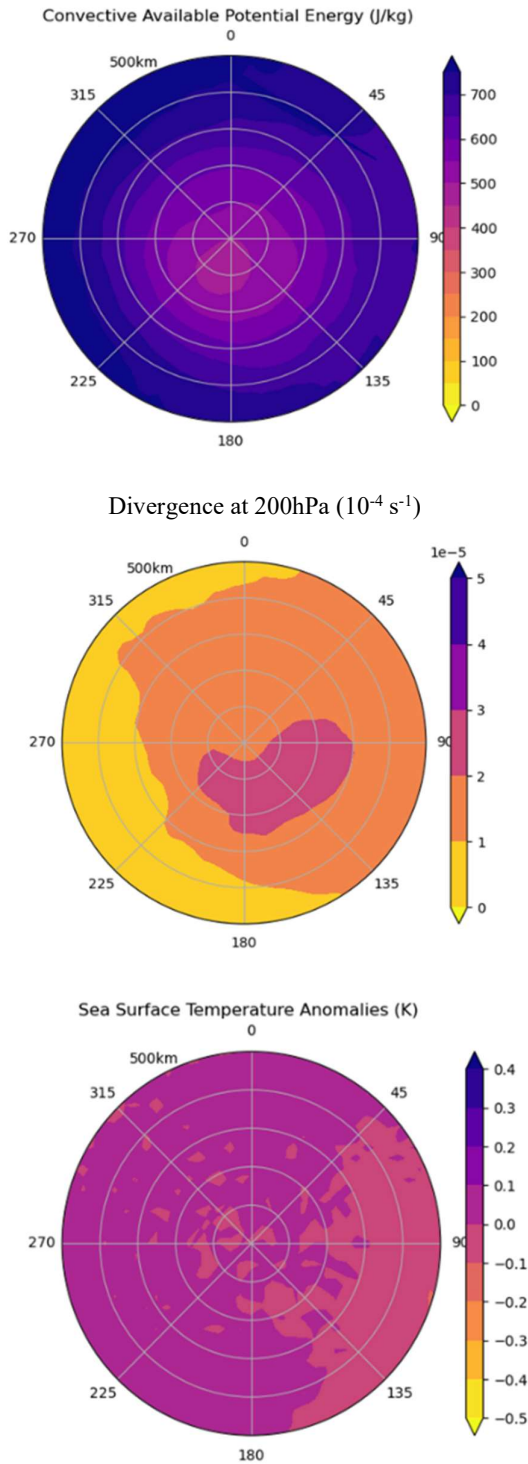


**Fig 14:** Excluded Features: CAPE(Topmost), Upper-Level Divergence (Middle)and SST anomalies (Below)

The Final features extracted are MSLP, Lower-level Vorticity, Total precipitation, Specific Humidity from 700hPa to 850hPa, Mean wind at 850hPa and 200hPa and Mean Wind shear between 850hPa and 200hPa. These features are averaged over the radius of maximum spatial correlation and considered for each cyclone data point. The data frame hence prepared is used for training the AI models.

### 3.1.2 Pearson's Correlation

The Pearson's correlation is calculated for the rotated and converted features with Vmax and the following values are shown below. Those which show the same correlation with both IMD and JTWC datasets are highlighted as positive/negative and those that have different signs with each of the datasets are categorised as inconclusive.

**Table 3:** Pearson's correlation Values

S No.	LARGE SCALE FEATURES	CORRELATION WITH VMAX		CORRELATION
		USING FEATURES	IMD	
1.	<b>Sea Surface Temperature</b>	<b>-0.019</b>	<b>0.13</b>	<b>INCONCLUSIVE</b>
2.	Mean Sea Level pressure	-0.08	-0.12	NEGATIVE
3.	Vorticity at 850 hPa	0.04	0.31	POSITIVE
4.	<b>Divergence at 200 hPa</b>	<b>0.05</b>	<b>0.06</b>	<b>POSITIVE</b>
5.	Total Precipitation	0.09	0.24	POSITIVE
6.	Specific Humidity- 700hPa	0.08	0.08	POSITIVE
7.	Specific Humidity - 750hPa	0.09	0.07	POSITIVE
8.	Specific Humidity -800hPa	0.1	0.05	POSITIVE

9.	Specific Humidity - 850hPa	0.1	0.07	POSITIVE
10.	Mean wind at 850hPa	0.22	0.56	POSITIVE
11.	Mean Wind at 200hPa	0.02	0.106	POSITIVE
12.	Mean Wind Shear between 850hPa and 200hPa	-0.09	-0.128	NEGATIVE
13.	CAPE	<b>0.06</b>	<b>0.17</b>	POSITIVE

The Spatial Heatmap of the 13 features with each other is shown in the figure below for each of the JTWC and IMD datasets (Fig15 and 16). Pearson's correlation values are able to successfully capture the relationship of the features with Vmax, except for the Specific Humidity from 700hPa-850hPa and Sea Surface Temperature. A positive correlation indicates that as the variable increases, Vmax is bound to increase and a Negative correlation indicates that as the variable increases, Vmax is bound to decrease. The low values of correlation tell us that the relation of the variables to Vmax is not independent, but a non-linear relationship between Vmax and the weighted combination of features.

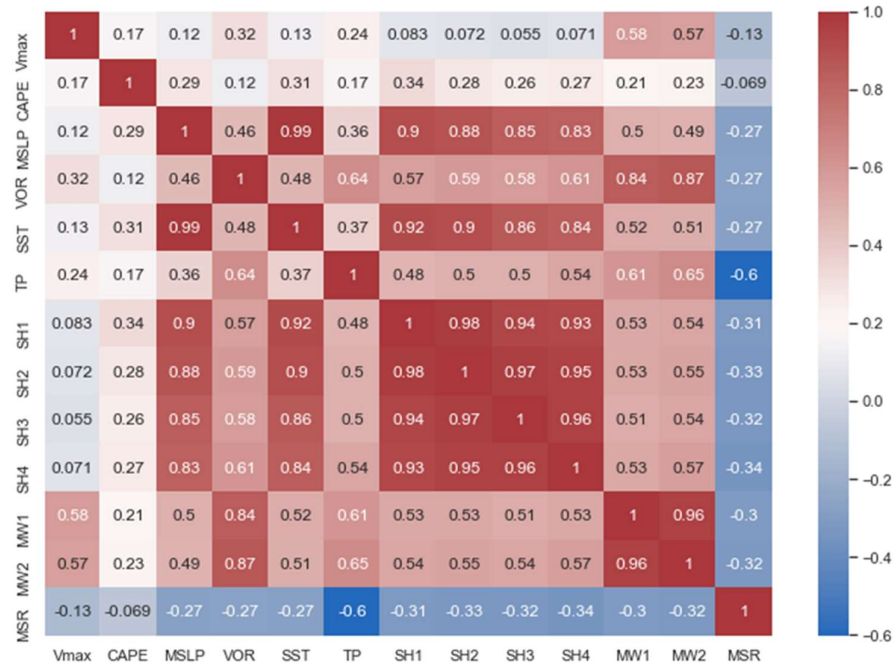


**Fig 15:** Correlation Heatmap of JTWC with respect to Vmax

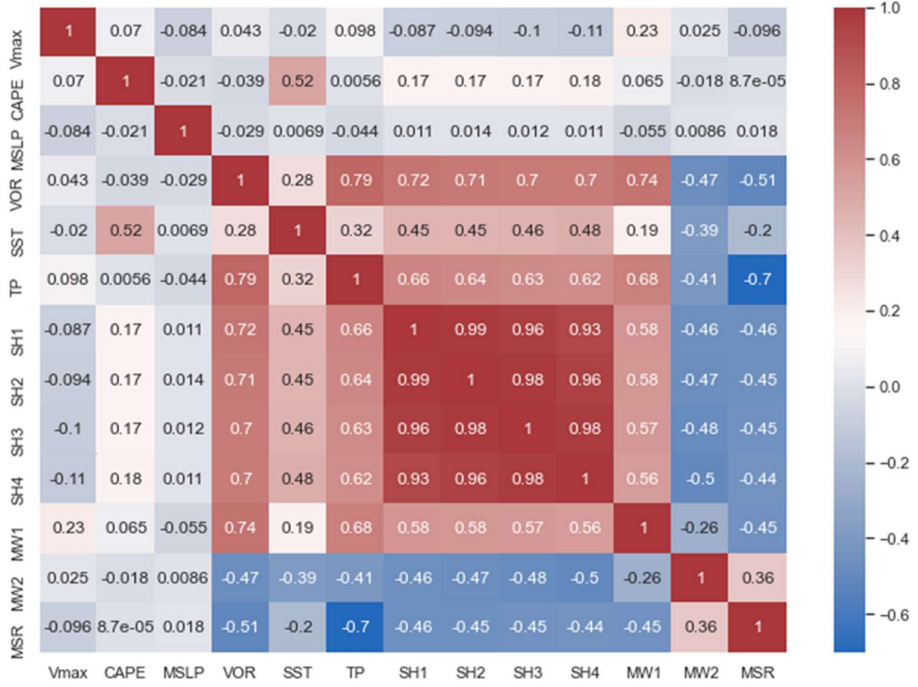


**Fig 16:** Correlation Heatmap of IMD with respect to Vmax

## 3.2 Machine Learning Model Simulation results

### **3.2.1 Random Forest (RF) Regressor**

The RF model predicts the 12 hr to 72 hr TC intensity using the IMD with lower bias and RMSE than that of JTWC. The best performance is achieved for the 12 hr and 24 hr TC intensity prediction. From the graph shown below (Fig 17) , the line depicts the mean of the intensity values predicted, for a particular Vmax value, with the spread indicating the error in prediction. The larger the spread, the more is the variance of predicted intensity values. The spread is narrower using the JTWC data forecasts when compared to IMD data forecasts.

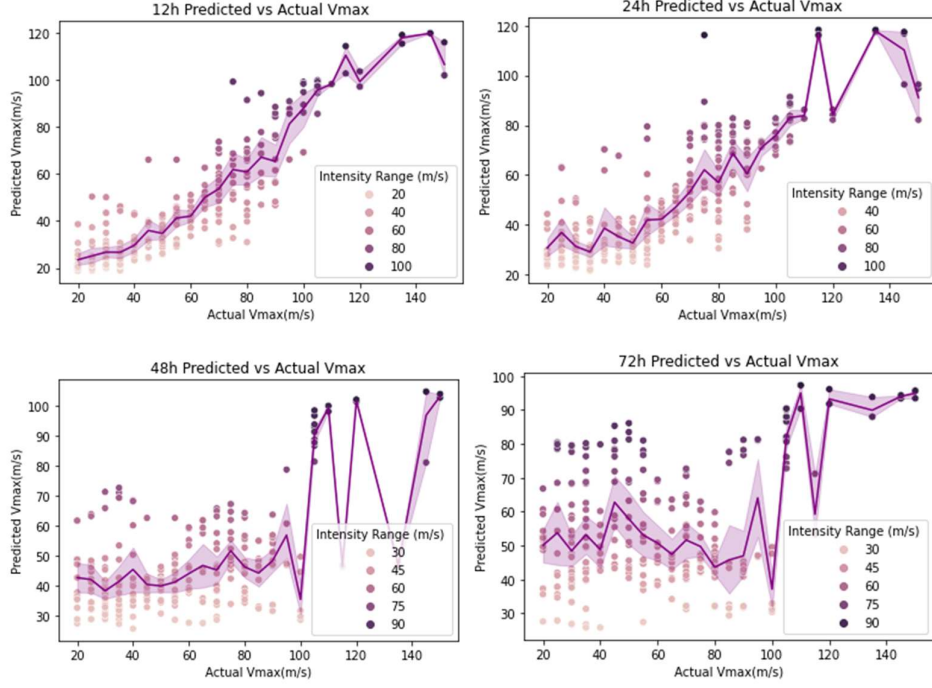


**Fig 17:** JTWC RF test data forecasts

**Table 4:** JTWC Error Metrics for RF

FORECAST HOUR	CORRELATION	RMSE (m/s)	BIAS (m/s)
12	0.90	17.45	-11.96
24	0.83	24.25	-12.12
48	-0.55	31.39	-14.44
72	-0.30	33.45	-8.55

Upon Comparing the Bias due to both the trained models, the bias is least for 12 hr, 24 hr, 48 hr, and 72 hr predictions using the IMD dataset (Fig 18). The model is also able to predict the lower intensity forecast values better than the higher intensity forecasts. The RF model is able to perform better using IMD data than JTWC due to the low mean error and higher mean correlation. The Correlation values are also positive and higher than JTWC, which shows a negative correlation for 48 hr and 72 hr forecasts. To improve the results, the SVM model was trained next.

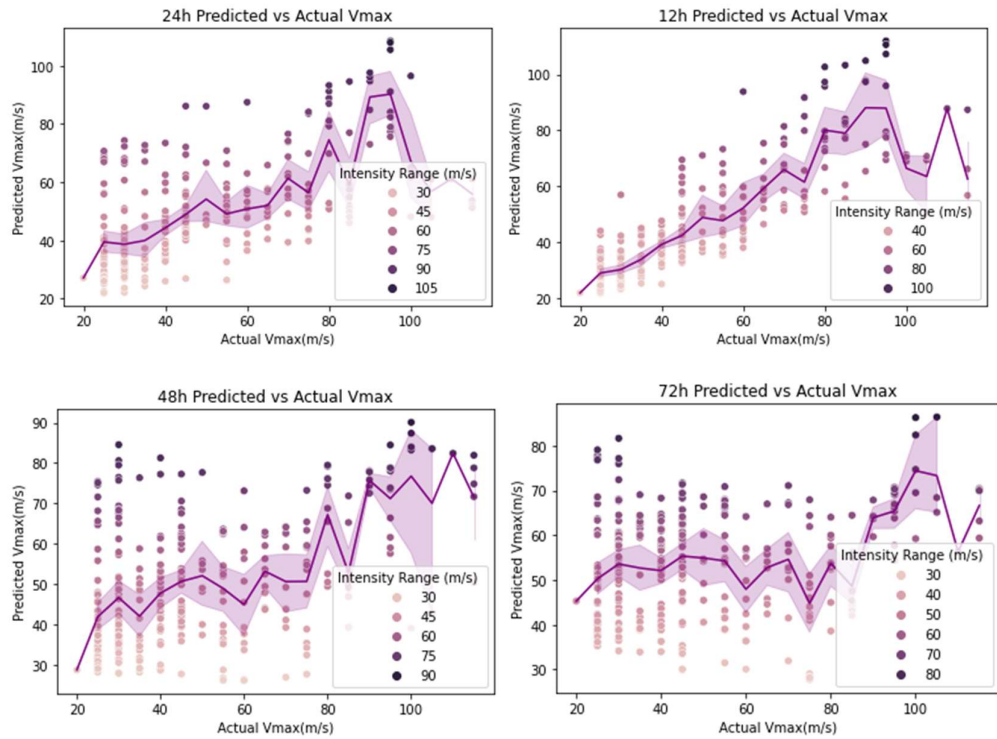


**Fig 18:** IMD RF test data forecasts

**Table 5:** IMD error metrics for RF

FORECAST HOUR	CORRELATION	RMSE (m/s)	BIAS(m/s)
12	0.83	12.39	-3.54
24	0.61	15.88	4.11
48	0.48	21.87	0.90
72	0.21	23.79	4.38

### 3.2.2 Support Vector Machines (SVM)

The SVM regressor showed better correlations using JTWC data than IMD Data, but lower error (RMSE/bias) using IMD data for each time step forecast (Fig 19 and 20). The spread of the variance is narrower for the JTWC predictions than that of IMD for 12 hr and 24 hr.

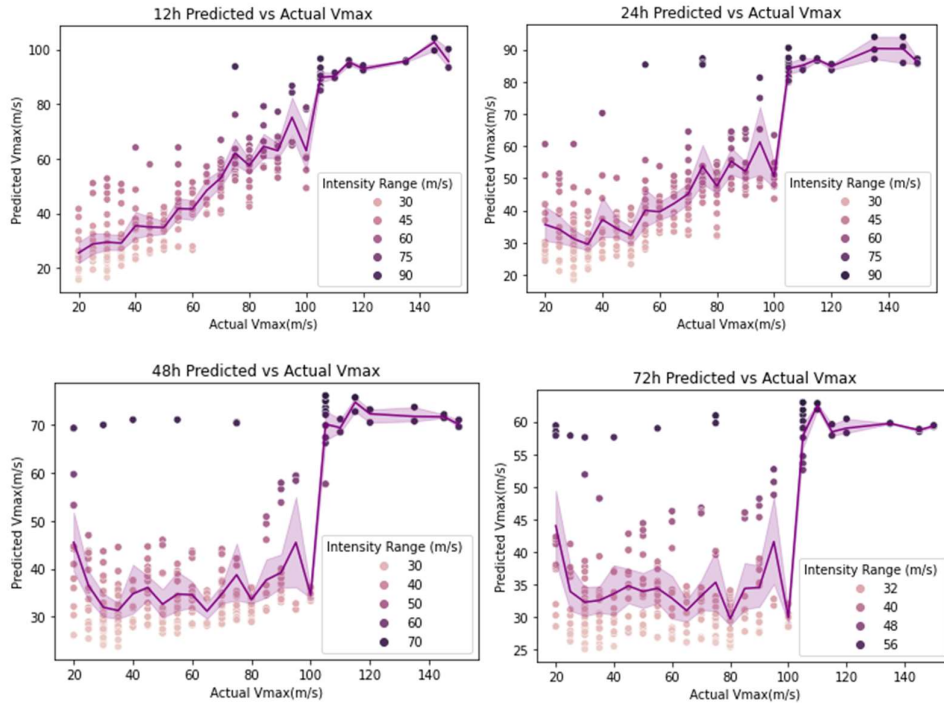


**Fig 19:** JTWC SVR test data forecasts

**Table 6:** JTWC Error Metrics for SVR

FORECAST HOUR	CORRELATION	RMSE (m/s)	BIAS (m/s)
12	0.90	18.37	-13.25
24	0.80	24.84	-16.84
48	0.53	33.41	-23.32
72	0.40	36.82	-26.28

Similarly, the lower intensity values are better predicted than the higher intensity ones due to the lack of availability of larger numbers of higher intensity data points. The 12 hr Correlation, RMSE and bias using JTWC data is (0.90, 18.37, -13.25) and for IMD is (0.84, -14.19, -5.76), significantly model trained with IMD data performs better.

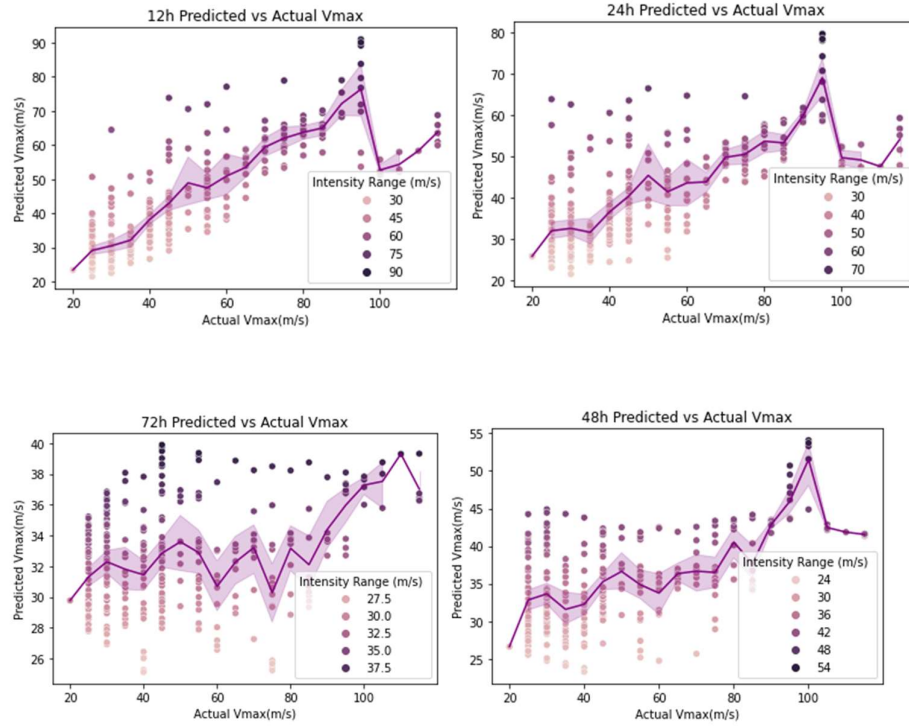


**Fig 20:** IMD SVR test data Forecasts

**Table 7:** IMD Error Metrics for SVR

FORECAST HOUR	CORRELATION	RMSE (m/s)	BIAS (m/s)
12	0.84	14.19	-5.76
24	0.73	19.19	-8.67
48	0.55	26.22	-13.84
72	0.29	29.32	-16.83

These Machine learning models directly learn from the data and features given. We can notice the constant negative bias in both the models using both datasets, indicating that the trained model is under-biased. But the errors are significant and due to the large dataset present, deep-learning models can be used to predict the TC intensity, which performs better with huge datasets.

### **3.3 Deep Learning Model LSTM Simulations results**

The summary of the LSTM model trained is given below. The model was initially tested for various ranges of Hyper Parameter values and the optimum value was deduced when the model had the least error. The model was run every 6 hours.

**Table 8:** LSTM Model Summary

HYPERPARAMETERS	RANGE OF HYPER-PARAMETERS TESTED	VALUE	OPTIMUM VALUE
Nodes	[50,100,150,200,500]	150	
Dropout	[0.10,0.20,0.30]	0.20	
Optimizer	['Adam','RMSprop','Adagrad','Adadelta','Adamax']	Adam (0.001 Learning rate)	
Activation	['relu','tanh']	Relu	
Epochs	[10,50,100,150,200]	200	
Batch size	[10,20,40,60,80,100]	20	

The LSTM model was then trained using both the datasets and the train and test loss curves were plotted (Fig 21 and 22). The loss is calculated based on the Mean absolute error (MAE) between the actual and the forecasts. With the number of Epochs increasing the loss must decrease, indicating that the model has learnt from the data and can predict with better accuracy. From the loss curves, LSTM has reduced the loss significantly from 30 m/s to 5m/s for the 12 hr and 24 hr forecasts for 200 epochs. But for 48 hr and 72 hr forecasts, the loss does

not drop below 25m/s using JTWC and 16m/s using IMD, which is significantly high. The performance of these models can be understood by running the model using the validation dataset.

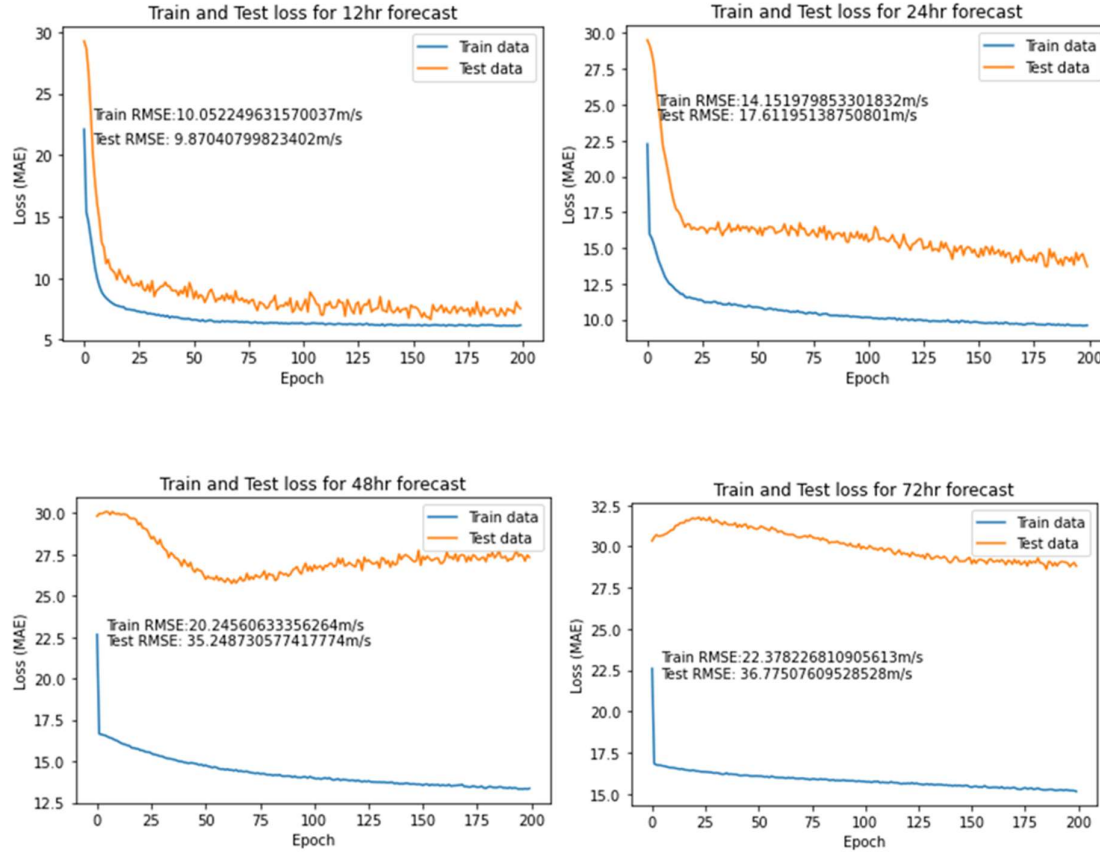


**Fig 21:** LSTM train and test loss curves for JTWC dataset

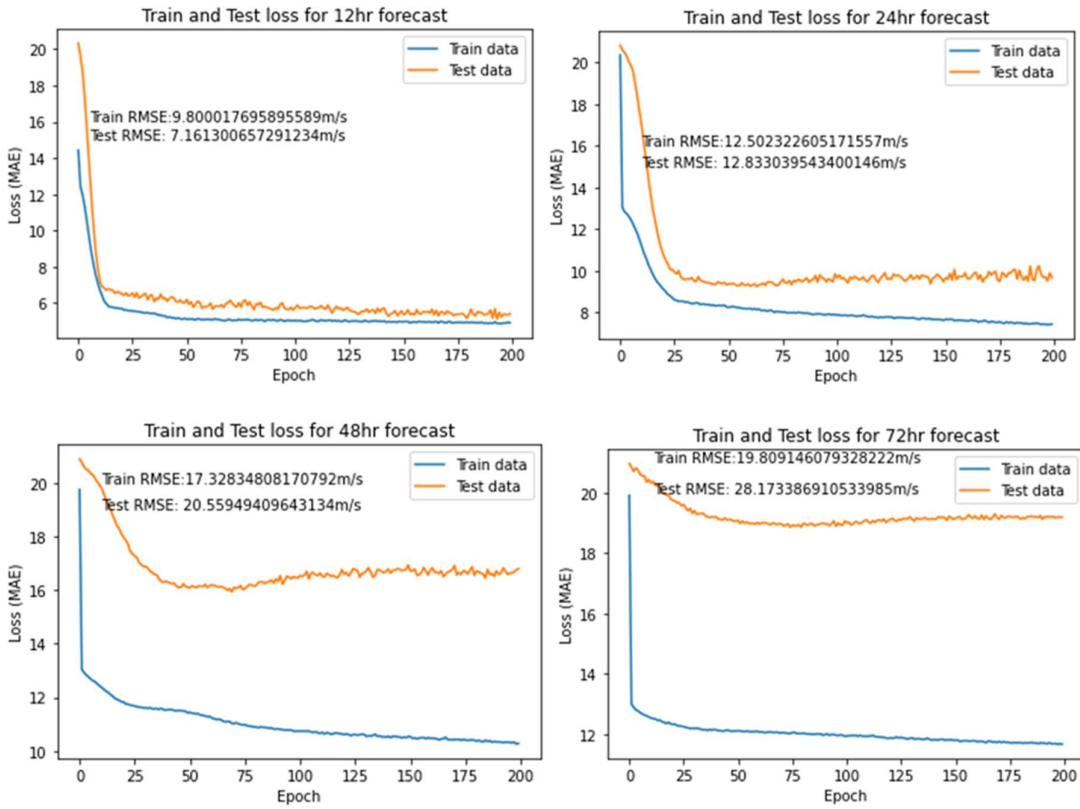


**Fig 22:** LSTM train and test loss curves for IMD dataset

Table 9 gives us the validation dataset used in the study to verify the performance of the model. The Name of the cyclone, Number of samples for each set of dates is mentioned for reference.

**Table 9:** Validation data: 2017 - 2019 for both IMD and JTWC datasets

S.No	Date Range	Number of Samples for each case	Name of the Cyclone
1.	2017-04-14 to 2017-04-17	12	MAARUTHA, BOB,
2.	2017-05-27 to 2017-05-30	20	MORA, BOB
3.	2017-11-28 to 2017-12-05	58	OCKHI, BOB
4.	2017-12-08 to 2017-12-10	7	Deep Depression, BOB

5.	2018-05-15 <b>to</b> 2018-05-27	72	MEKUNU, AS
6.	2018-05-28 <b>to</b> 2018-05-30	8	Deep Depression, BOB
7.	2018-09-19 <b>to</b> 2018-09-21	7	DAYE, BOB
8.	2018-11-10 <b>to</b> 2018-11-19	40	GAJA, BOB
9.	2018-12-13 <b>to</b> 2018-12-17	18	PHETHAI, BOB
10.	2019-04-25 <b>to</b> 2019-05-04	70	FANI, BOB
11.	2019-09-20 <b>to</b> 2019-09-26	33	HIKKA, AS
<b>Total Number of Data points</b>		<b>345</b>	

The 6 hr to 72 hr TC intensity predictions were performed using both the datasets and the results are summarised for 12 hr, 24 hr, 48 hr and 72 hr predictions (Fig 23 and 24). Consistent with the previous results, the plots for 12 hr and 24 hr predictions indicate that the pattern is similar to the actual intensities with the least mean bias with the IMD dataset (1.9m/s, -2.22m/s) respectively for 12 hr and 24 hr forecasts, which is significantly lesser than the RF and SVM regression models. The same using the JTWC dataset is also low but higher than the IMD results. The 48 hr and 72 hr predictions using IMD data have reduced error significantly when compared to RF and SVM forecasts with a bias of -9.71 m/s and 15.71 m/s respectively for 12 hr and 24 hr forecasts. Though there is scope for better performance in the longer-range predictions, the 12 hr and 24 hr predictions have very high accuracy.

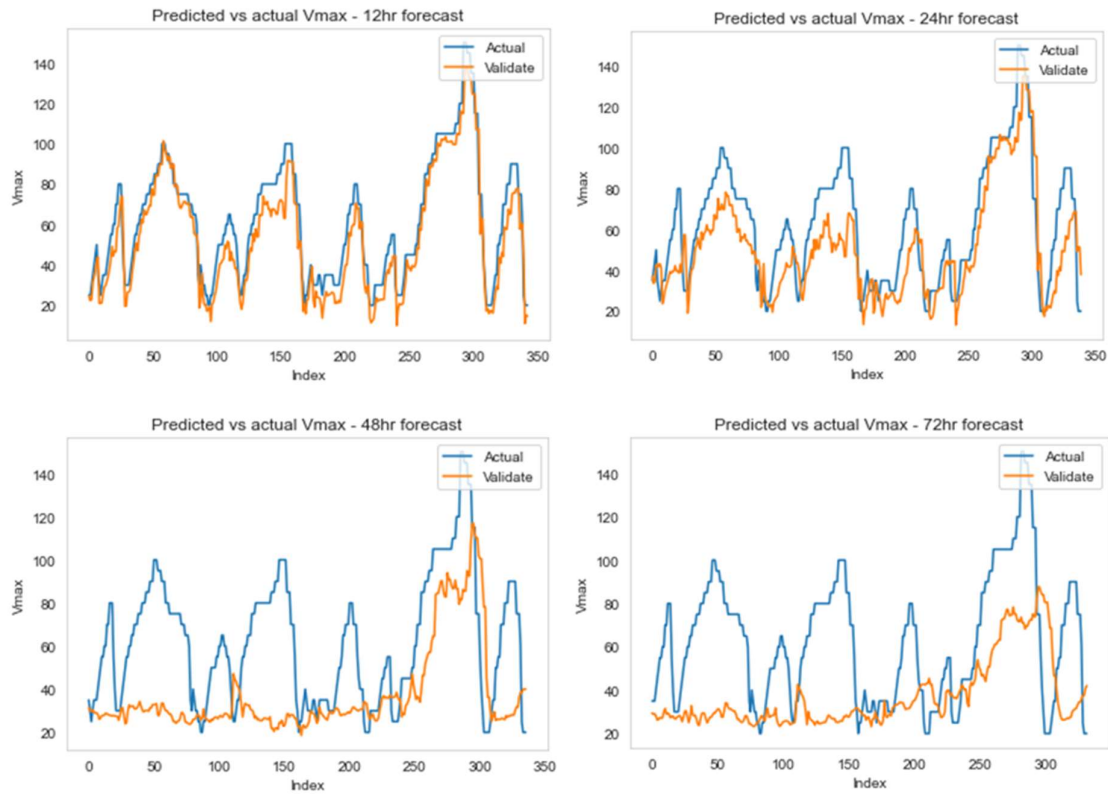


**Fig 23:** LSTM Actual and Predicted Vmax for JTWC dataset

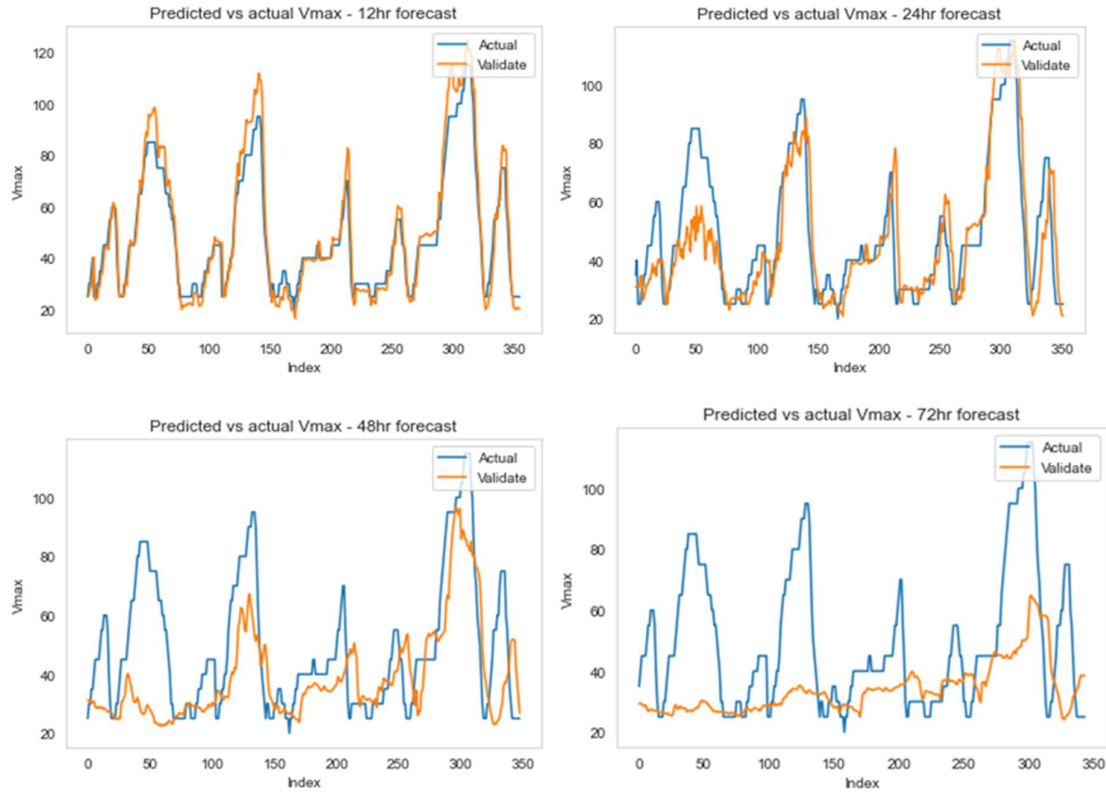


**Fig 24:** LSTM Actual and Predicted Vmax for IMD dataset

In order to compare the performance between the two datasets, the distribution plot of the bias is plotted (Fig 25). The maximum density in the IMD dataset is centred around 0m/s, for 12 hr to 72 hr predictions indicating that the maximum number of predictions has very least bias. Whereas with the JTWC dataset, the maximum density is centred around -20m/s for 12 hr and 24 hr predictions and the rest are widely distributed and there is no maximum peak found. This indicates that the IMD dataset has trained the model better than the JTWC dataset and such a model is more reliable due to the least error.

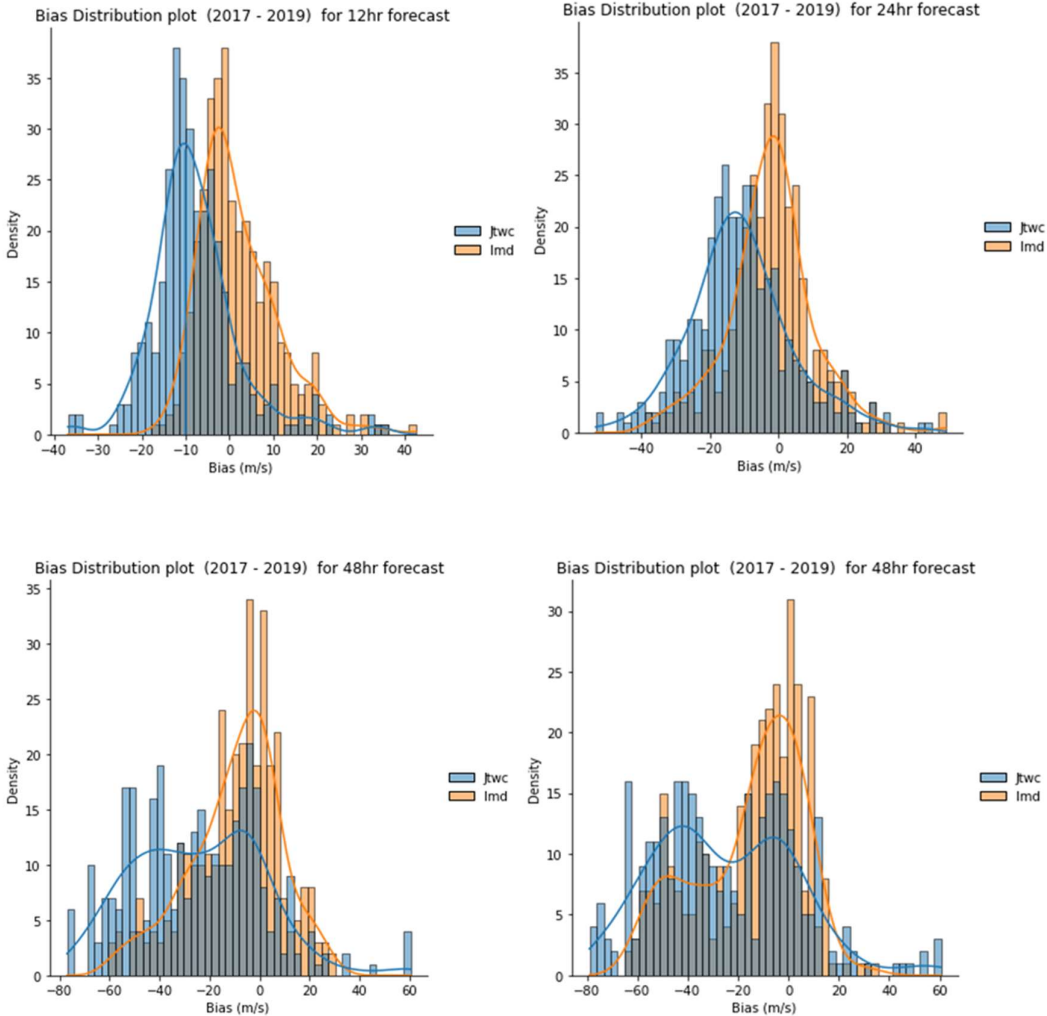


**Fig 25:** Comparison of Distribution of Bias between actual and Predicted Vmax

In order to analyse deeper, the bias is plotted as a box plot for each cyclone due to both IMD and JTWC trained models for 12 hr, 24 hr, 48 hr and 72 hr forecasts (Fig 26 and 27). The common observation using both the trained models is that the 12hr prediction bias is the least when compared to other time step predictions. The least bias is found for DAYE and OCKHI cyclones respectively for JTWC and IMD models. The maximum bias is found for the MEKUNU cyclone using both models. The bias in the 12 hr predicting model is very close to the zero line. For the 24-hr prediction, the model trained using IMD performs much better than JTWC due to a lower bias for each of the cyclone. The overall bias is lower using IMD when compared to JTWC.

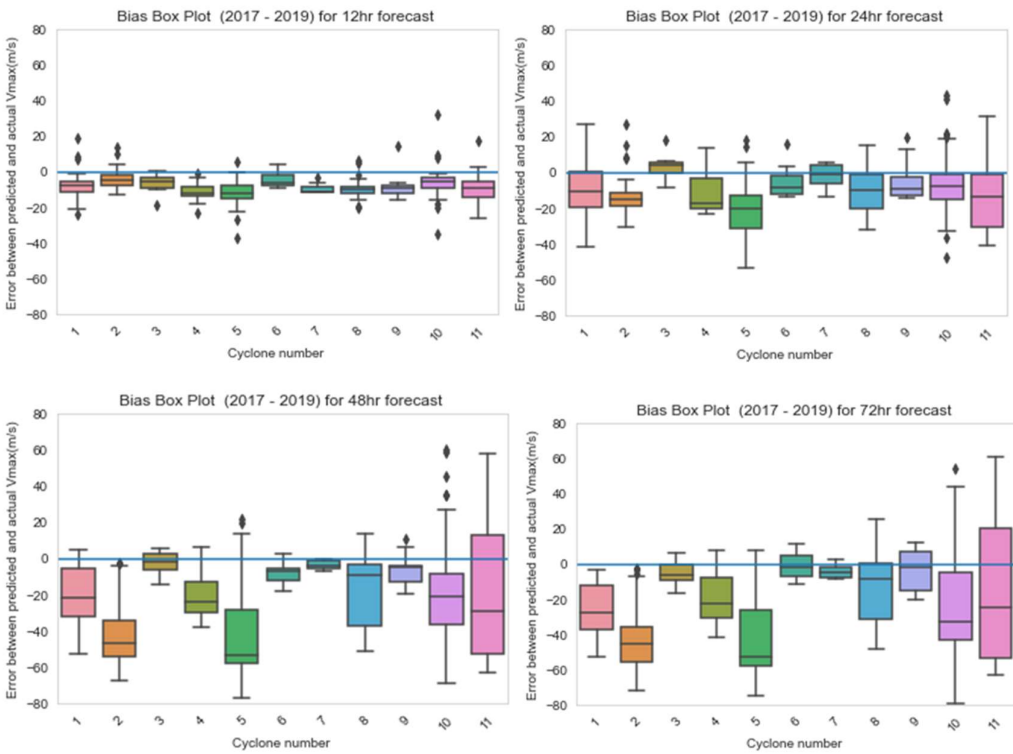


**Fig 26:** Bias Box plot for JTWC validation dataset for each cyclone

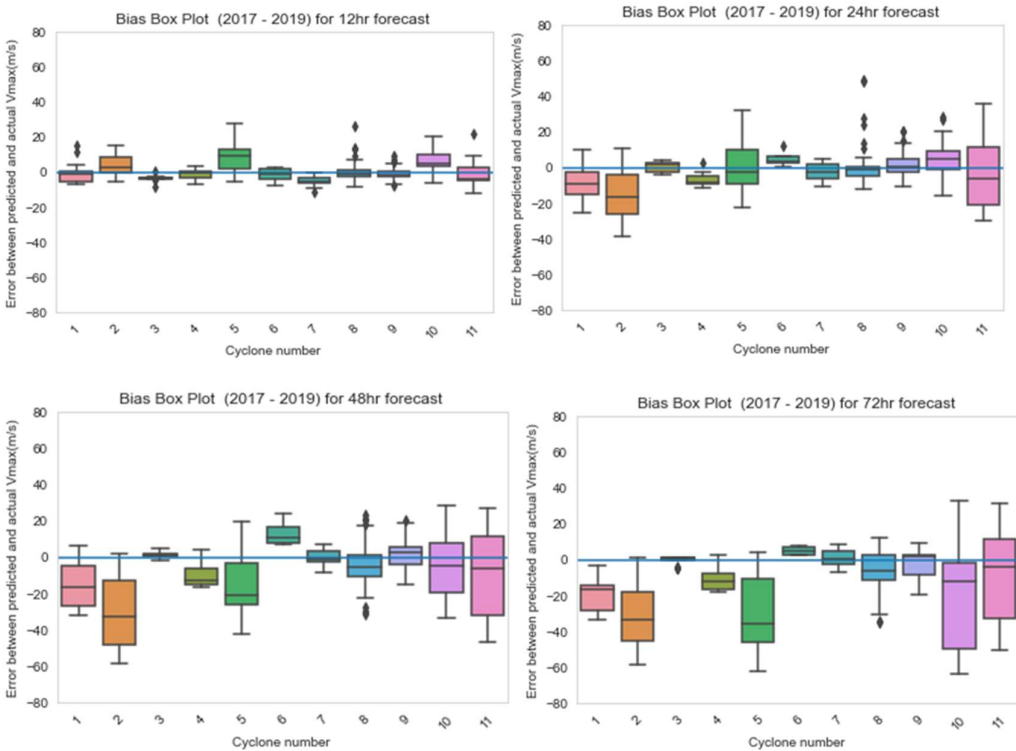


**Fig 27:** Bias Box plot for IMD validation dataset for each cyclone

The error statistics - correlation, bias and RMSE of each validation run using IMD and JTWC trained models are summarised in Tables 10 and 11.

**Table 10:** Error statistics against IMD dataset

FORECAST HOUR	CORRELATION	RMSE (m/s)	BIAS(m/s)
6	0.98	8.46	3.32
12	0.95	9.16	1.9
18	0.91	10.14	1.22
24	0.84	12.83	-2.22
30	0.72	16.92	-4.24
36	0.66	18.50	-5.59
42	0.63	19.65	-7.75
48	0.61	20.55	-9.71
54	0.56	21.56	-10.49
60	0.52	22.72	-11.88
66	0.45	24.33	-13.47
72	0.38	25.97	-15.31

We can conclude that the model is able to perform very well for 6 hr, 12 hr, 18 hr and 24 hr predictions. The model trained using IMD performs significantly better than the model trained using JTWC. The 72-hr prediction using both models has a large error, though the correlation is positive.

**Table 11:** Error statistics against the JTWC dataset

FORECAST HOUR	CORRELATION	RMSE ( <i>m/s</i> )	BIAS ( <i>m/s</i> )
6	0.97	11.86	-9.84
12	0.94	12.70	-7.90
18	0.91	14.43	-8.4
24	0.85	18.6	-11.01
30	0.7	28.06	-18.65
36	0.62	32.01	-21.95
42	0.56	34.23	-23.77
48	0.51	35.78	-24.69
54	0.48	36.16	-24.80
60	0.45	36.67	-25.09
66	0.39	37.86	-25.86
72	0.36	37.65	-25.36

The scatter plot was plotted between the actual and forecast Vmax values for 12 hr, 24 hr, 48 hr and 72 hr predictions using both the trained models (Fig 28 ad 29). The correlation is highest for 12hr and 24hr predictions using both the trained models and greater than 0.5 for 12 hr to 48 hr predictions. A strong correlation with a constant bias means that the model is biased uniformly and can be corrected. The correlation, bias and RMSE for each forecast run using both the type of models trained with IMD and JTWC dataset are plotted (Fig 30,31,32). The correlation is found to be the same till 36hr forecasts for IMD and JTWC trained and the correlation further drops for JTWC when compared to IMD for 36 hr to 72 hr predictions. The mean bias plot indicates that the JTWC trained model has a very high bias when compared to IMD trained. Lower bias in the IMD trained models indicates better accuracy. The difference may be attributed to the observation data difference between JTWC and IMD. The RMSE plot

is also similar to that of bias, with the model trained using IMD having significantly lower error when compared to JTWC.

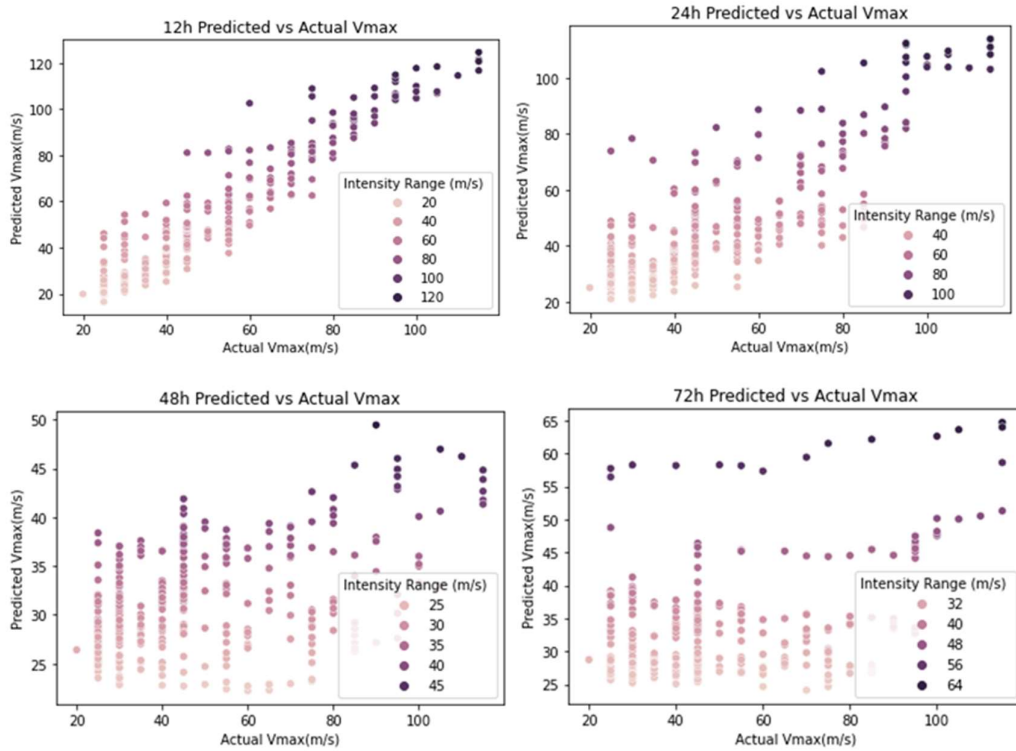


**Fig 28:** Scatter plots between actual and forecast Vmax for JTWC dataset

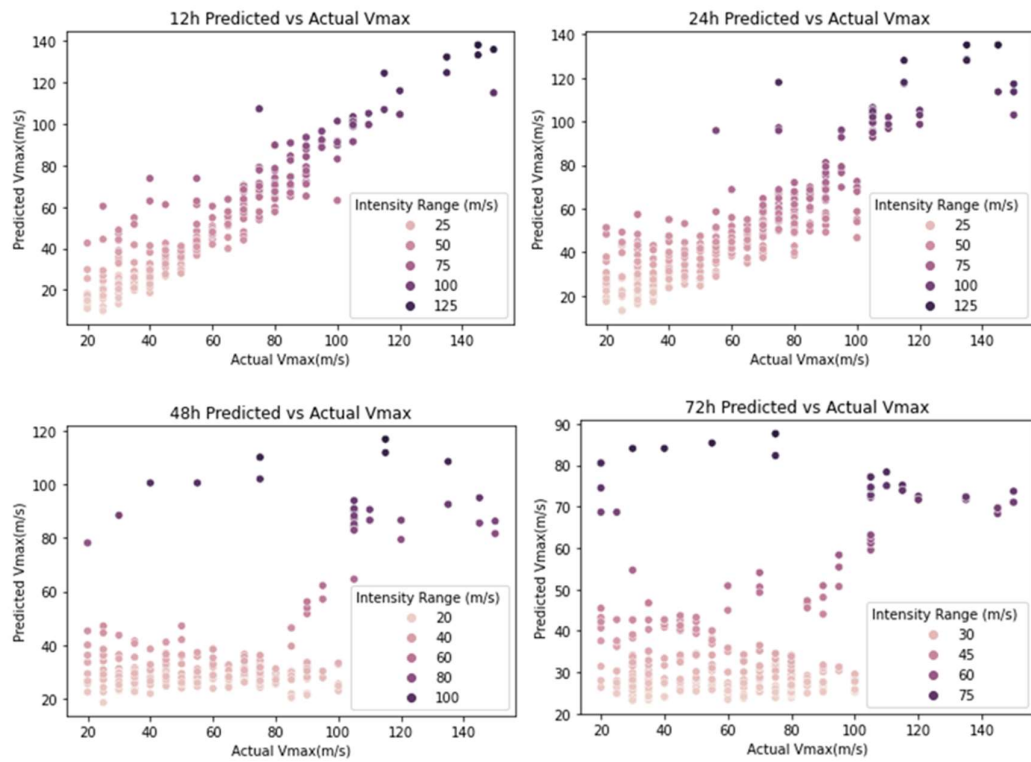


**Fig 29:** Scatter plots between actual and forecast Vmax for IMD dataset

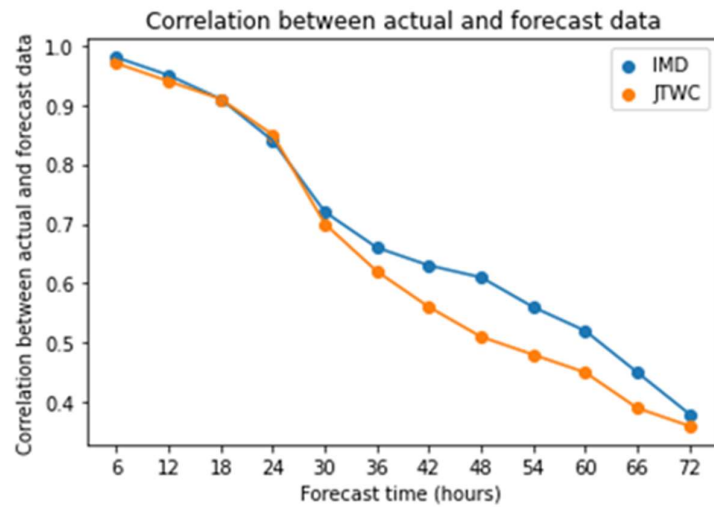


**Fig 30:** Correlation between actual and forecast Vmax for IMD and JTWC datasets

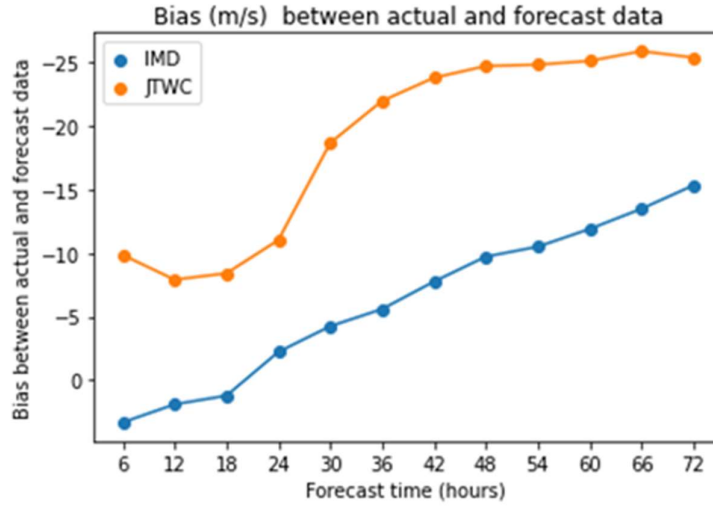


**Fig 31:** Bias between actual and forecast Vmax for IMD and JTWC datasets

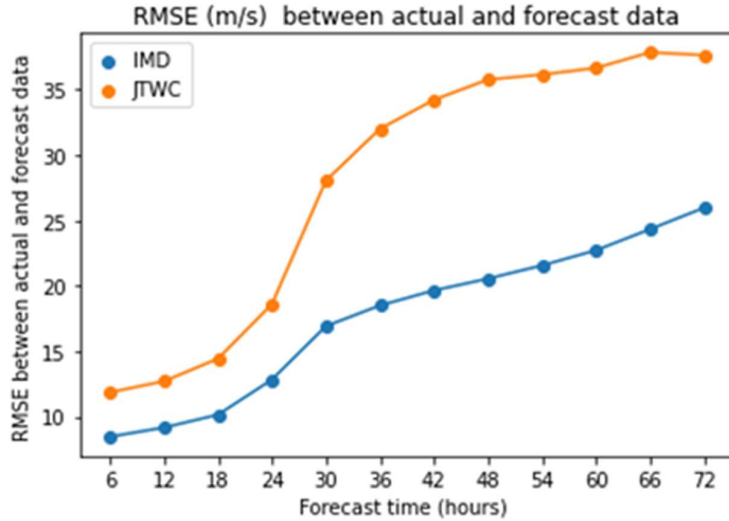


**Fig 32:** RMSE between actual and forecast Vmax for IMD and JTWC datasets

In order to summarise the performance of the three models, the coefficients are shown in Table 12 for models trained using IMD and JTWC datasets. We can notice in the datasets, how the shift from Machine learning to deep learning models has significantly increased the correlation and reduced the bias and RMSE in both the cases.

**Table 12:** Error Statistics summary for intensity prediction (Vmax) for IMD and JTWC dataset

TC centre considered	FORECAST HOUR	Support Vector Machine regressor			Random Forest Regressor			LSTM		
		Correlation	RMSE (m/s)	Bias (m/s)	Correlation	RMSE (m/s)	Bias (m/s)	Correlation	RMSE (m/s)	Bias (m/s)
IMD	12	0.84	14.19	-5.76	0.83	12.39	-3.54	0.95	9.16	1.9
	24	0.73	19.19	-8.67	0.61	15.88	0.11	0.84	12.83	-2.22
	48	0.55	26.22	-13.84	0.48	21.87	0.90	0.61	20.55	-9.71
	72	0.29	29.32	-16.83	0.21	23.79	4.38	0.38	25.97	-15.31
JTWC	12	0.90	18.37	-13.25	0.90	17.45	-11.96	0.94	12.70	-7.90
	24	0.80	24.84	-16.84	0.83	24.25	-12.12	0.85	18.6	-11.01
	48	0.53	33.41	-23.32	-0.55	31.39	-14.44	0.51	35.78	-24.69
	72	0.40	36.82	-26.82	-0.30	33.45	-8.55	0.36	37.65	-25.36

For a 12-hr forecast, the LSTM model trained using IMD data performs the best and can give the best forecast accurately. For a 24-hr forecast, similarly, LSTM trained using IMD data can give accurate forecasts. For 48hr forecasts, the LSTM trained using IMD data performs the best. For 72 hr forecasts, the LSTM trained using IMD data performs the best.

# **Chapter 4**

## **Conclusions**

The climatology plots and the Pearson's correlation for the various features were used for extracting 10 features correlated with TC intensification. Comparing the SVM, RF, and LSTM model for the IMD data-frame, LSTM performed the best with the highest correlation and least error (Bias/ RMSE) for 12 hr to 72 hr forecasts. Comparing the above models for the JTWC dataset, LSTM performed the best for 12 hr and 24 hr forecasts, with the highest correlation and least error.

TC intensity is accurately predicted for the next 12 hr and 24 hr forecasts, with a mean bias of -3 m/s for 12 hr forecast and 6.6m/s for 24 hr forecast. Upon comparing the IMD and JTWC datasets based on the density of the bias distribution, IMD is more accurate as the maximum density of bias is located around 0 when compared to JTWC.

The LSTM train and test loss curves suggest that the test error is the least when used with IMD data frames for 12 hr and 24 hr forecasts, whereas the 48 hr and 72 hr forecast error is very significant for both IMD and JTWC data frames. The lower the test error, the better the accuracy of the model trained.

The bias box plots depicting the error for each cyclone suggest that for 12hr and 24hr forecasts, the model has a bias close to zero for 12 hr forecasts using both datasets. The minimum bias is predicted for the Daye cyclone, BOB, and the maximum bias for the Mekunu Cyclone, AS.

The 6 hr to 72 hr single step TC intensity LSTM runs suggest that the bias is significantly higher in JTWC than in IMD. The correlation is similar up to 36 hr forecasts but becomes higher for IMD henceforth. Though the RMSE is high, the strong correlation value indicates that the bias is constant (Spread) and bias correction can be performed for better forecast accuracy. Hence, the LSTM model can be used to predict the TC intensity for the next 12hr and 24hr with the best forecast accuracy. The LSTM model, hence, trained using IMD data performs the best for 6 hr to 72 hr forecasts when compared to other models and gives highly accurate predictions of TC intensity for the next 6 hr, 12 hr, 24 hr time steps.

## **Scopes for Further Research**

This study primarily used ERA5 reanalysis data as a source for its variables. The quality of the data used for feature extraction can be improved. The number of features used in this study is 10, and this can also be increased further and better feature extraction methods can be deployed. The data can be biased and bias correction methods can be implemented in order to eliminate the bias from the data and its outputs. Further, the work can be extended to analyse the rapid intensification of Tropical cyclones.

## References

Ankur, Kumar, et al. "On the relationship between intensity changes and rainfall distribution in tropical cyclones over the North Indian Ocean." *International journal of climatology* 40.4 (2020): 2015-2025.

Balaguru, K., Foltz, G. R., Leung, L. R., Hagos, S. M., & Judi, D. R. (2018). On the Use of Ocean Dynamic Temperature for Hurricane Intensity Forecasting. In *Weather and Forecasting* (Vol. 33, Issue 2, pp. 411–418). American Meteorological Society. <https://doi.org/10.1175/waf-d-17-0143.1>

Balachandran, S., Nadimpalli, R., Osuri, K. K., Marks, F. D., Gopalakrishnan, S., Subramanian, S., Mohanty, U. C., & Niyogi, D. (2019). On the processes influencing rapid intensity changes of tropical cyclones over the Bay of Bengal. In *Scientific Reports* (Vol. 9, Issue 1). Springer Science and Business Media LLC. <https://doi.org/10.1038/s41598-019-40332-z>

Cangialosi, J. P., Blake, E., DeMaria, M., Penny, A., Latto, A., Rappaport, E., & Tallapragada, V. (2020). Recent Progress in Tropical Cyclone Intensity Forecasting at the National Hurricane Center. In *Weather and Forecasting* (Vol. 35, Issue 5, pp. 1913–1922). American Meteorological Society. <https://doi.org/10.1175/waf-d-20-0059.1>

Chaudhuri, S., Dutta, D., Goswami, S., & Middey, A. (2012). Intensity forecast of tropical cyclones over North Indian Ocean using multilayer perceptron model: skill and performance verification. In *Natural Hazards* (Vol. 65, Issue 1, pp. 97–113). Springer Science and Business Media LLC. <https://doi.org/10.1007/s11069-012-0346-7>

Chaudhuri, S., Dutta, D., Goswami, S., & Middey, A. (2012). Intensity forecast of tropical cyclones over North Indian Ocean using multilayer perceptron model: skill and performance verification. In *Natural Hazards* (Vol. 65, Issue 1, pp. 97–113). Springer Science and Business Media LLC. <https://doi.org/10.1007/s11069-012-0346-7>

Chen, R., Wang, X., Zhang, W., Zhu, X., Li, A., & Yang, C. (2019). A hybrid CNN-LSTM model for typhoon formation forecasting. In *GeoInformatica* (Vol. 23, Issue 3, pp. 375–396). Springer Science and Business Media LLC. <https://doi.org/10.1007/s10707-019-00355-0>

Chen, R., Wang, X., Zhang, W., Zhu, X., Li, A., & Yang, C. (2019). A hybrid CNN-LSTM model for typhoon formation forecasting. In *GeoInformatica* (Vol. 23, Issue 3, pp. 375–396). Springer Science and Business Media LLC. <https://doi.org/10.1007/s10707-019-00355-0>

Chen, R., Zhang, W., & Wang, X. (2020). Machine Learning in Tropical Cyclone Forecast Modeling: A Review. In *Atmosphere* (Vol. 11, Issue 7, p. 676). MDPI AG. <https://doi.org/10.3390/atmos11070676>

Cloud, K. A., Reich, B. J., Rozoff, C. M., Alessandrini, S., Lewis, W. E., & Delle Monache, L. (2019). A Feed Forward Neural Network Based on Model Output Statistics for Short-Term Hurricane Intensity Prediction. In *Weather and Forecasting* (Vol. 34, Issue 4, pp. 985–997). American Meteorological Society. <https://doi.org/10.1175/waf-d-18-0173.1>

Fudeyasu, H., & Wang, Y. (2011). Balanced Contribution to the Intensification of a Tropical Cyclone Simulated in TCM4: Outer-Core Spinup Process\*. In *Journal of the Atmospheric Sciences* (Vol. 68, Issue 3, pp. 430–449). American Meteorological Society. <https://doi.org/10.1175/2010jas3523.1>

Gray, W. M. (1979). Hurricanes: Their formation, structure and likely role in the tropical circulation, *Meteorology over the tropical oceans*, 77, 155-218.

Ito, K. (2016). Errors in Tropical Cyclone Intensity Forecast by RSMC Tokyo and Statistical Correction Using Environmental Parameters. In *SOLA* (Vol. 12, Issue 0, pp. 247–252). Meteorological Society of Japan. <https://doi.org/10.2151/sola.2016-049>

J.-J. Baik, J.-S. Paek, A neural network model for predicting typhoon intensity, *J. Meteorol. Soc. Jpn.* 78 (2000) 857–869, [http://dx.doi.org/10.2151/jmsj1965.78.6\\_857](http://dx.doi.org/10.2151/jmsj1965.78.6_857)

Kaplan, J., Rozoff, C. M., DeMaria, M., Sampson, C. R., Kossin, J. P., Velden, C. S., Cione, J. J., Dunion, J. P., Knaff, J. A., Zhang, J. A., Dostalek, J. F., Hawkins, J. D., Lee, T. F., & Solbrig, J. E. (2015). Evaluating Environmental Impacts on Tropical Cyclone Rapid Intensification Predictability Utilizing Statistical Models. In *Weather and Forecasting* (Vol. 30, Issue 5, pp. 1374–1396). American Meteorological Society. <https://doi.org/10.1175/waf-d-15-0032.1>

Kotal, S. D., et al. "A statistical cyclone intensity prediction (SCIP) model for the Bay of Bengal." *Journal of earth system science* 117.2 (2008): 157-168.

Kotal, S.D. & Bhowmik, S.K.. (2013). Large-scale characteristics of rapidly intensifying tropical cyclones over the Bay of Bengal and a Rapid Intensification (RI) index. *Mausam*. 64. 13-24.

Kumar, S., Biswas, K., & Pandey, A. K. (2021). Prediction of Landfall Intensity, Location, and Time of a Tropical Cyclone (Version 1). arXiv. <https://doi.org/10.48550/ARXIV.2103.16180>

Lee, C.-Y., Tippett, M. K., Sobel, A. H., & Camargo, S. J. (2016). Rapid intensification and the bimodal distribution of tropical cyclone intensity. In *Nature Communications* (Vol. 7, Issue 1). Springer Science and Business Media LLC. <https://doi.org/10.1038/ncomms10625>

Li, Q., Li, Z., Peng, Y., Wang, X., Li, L., Lan, H., Feng, S., Sun, L., Li, G., & Wei, X. (2018). Statistical Regression Scheme for Intensity Prediction of Tropical Cyclones in the Northwestern Pacific. In *Weather and Forecasting* (Vol. 33, Issue 5, pp. 1299–1315). American Meteorological Society. <https://doi.org/10.1175/waf-d-18-0001.1>

Liu, & Bo Feng. (2005). A neural network regression model for tropical cyclone forecast. In 2005 International Conference on Machine Learning and Cybernetics. Proceedings of 2005 International Conference on Machine Learning and Cybernetics. IEEE. <https://doi.org/10.1109/icmlc.2005.1527659>

Liu, B. Feng, A neural network regression model for tropical cyclone forecast, in: 2005 International Conference on Machine Learning and Cybernetics, Vol. 7, 2005, pp. 4122–4128, <http://dx.doi.org/10.1109/ICMLC.2005.1527659>.

Nadimpalli, R., Mohanty, S., Pathak, N., Osuri, K. K., Mohanty, U. C., & Chatterjee, S. (2021). Understanding the characteristics of rapid intensity changes of Tropical Cyclones over North Indian Ocean. In *SN Applied Sciences* (Vol. 3, Issue 1). Springer Science and Business Media LLC. <https://doi.org/10.1007/s42452-020-03995-2>

Nadimpalli, R., Mohanty, S., Pathak, N., Osuri, K. K., Mohanty, U. C., & Chatterjee, S. (2021). Understanding the characteristics of rapid intensity changes of Tropical Cyclones over North Indian Ocean. In *SN Applied Sciences* (Vol. 3, Issue 1). Springer Science and Business Media LLC. <https://doi.org/10.1007/s42452-020-03995-2>

Noble, W. S. (2006). What is a support vector machine? In *Nature Biotechnology* (Vol. 24, Issue 12, pp. 1565–1567). Springer Science and Business Media LLC. <https://doi.org/10.1038/nbt1206-1565>

Osuri, K. K., Mohanty, U. C., Routray, A., Mohapatra, M., & Niyogi, D. (2013). Real-Time Track Prediction of Tropical Cyclones over the North Indian Ocean Using the ARW Model. In *Journal of Applied Meteorology and Climatology* (Vol. 52, Issue 11, pp. 2476–2492). American Meteorological Society. <https://doi.org/10.1175/jamc-d-12-0313.1>

Pan, B., Xu, X., & Shi, Z. (2019). Tropical cyclone intensity prediction based on recurrent neural networks. In *Electronics Letters* (Vol. 55, Issue 7, pp. 413–415). Institution of Engineering and Technology (IET). <https://doi.org/10.1049/el.2018.8178>

Pan, B., Xu, X., & Shi, Z. (2019). Tropical cyclone intensity prediction based on recurrent neural networks. In *Electronics Letters* (Vol. 55, Issue 7, pp. 413–415). Institution of Engineering and Technology (IET). <https://doi.org/10.1049/el.2018.8178>.

Rao, Y. P. (1976). Southwest Monsoon, IMD, Met. Monograph No. Synoptic Meteorology—1/76. Rathore, L. S., Mohapatra, M., & Geetha, B. (2017). Collaborative Mechanism for Tropical Cyclone Monitoring and Prediction over North Indian Ocean. In *Tropical Cyclone Activity over the North Indian Ocean* (pp. 3-27). Springer International Publishing.

Rappaport, E. N., Jiing, J.-G., Landsea, C. W., Murillo, S. T., & Franklin, J. L. (2012). The Joint Hurricane Test Bed: Its First Decade of Tropical Cyclone Research-To-Operations Activities Reviewed. In *Bulletin of the American Meteorological Society* (Vol. 93, Issue 3, pp. 371–380). American Meteorological Society. <https://doi.org/10.1175/bams-d-11-00037.1>

Schonlau, M., & Zou, R. Y. (2020). The random forest algorithm for statistical learning. In *The Stata Journal: Promoting communications on statistics and Stata* (Vol. 20, Issue 1, pp. 3–29). SAGE Publications. <https://doi.org/10.1177/1536867x20909688>

Su, H., Wu, L., Jiang, J. H., Pai, R., Liu, A., Zhai, A. J., Tavallali, P., & DeMaria, M. (2020). Applying Satellite Observations of Tropical Cyclone Internal Structures to Rapid

Intensification Forecast With Machine Learning. In *Geophysical Research Letters* (Vol. 47, Issue 17). American Geophysical Union (AGU). <https://doi.org/10.1029/2020gl089102>

Vinodhkumar, B., Busireddy, N. K. R., Ankur, K., Nadimpalli, R., & Osuri, K. K. (2021). On occurrence of rapid intensification and rainfall changes in tropical cyclones over the North Indian Ocean. In *International Journal of Climatology* (Vol. 42, Issue 2, pp. 714–726). Wiley. <https://doi.org/10.1002/joc.7268>

Wenwei, X., Karthik, B., Andrew, A., Nicholas, L., Nathan, H., Mark, D., & David, J. (2021). Deep Learning Experiments for Tropical Cyclone Intensity Forecasts. In *Weather and Forecasting*. American Meteorological Society. <https://doi.org/10.1175/waf-d-20-0104.1>

X. Yi, J. Zhang, Z. Wang, T. Li, Y. Zheng, Deep distributed fusion network for air quality prediction, in: Proceedings of the 24th ACM SIGKDD International Conference on Knowledge Discovery & Data Mining, ACM, London United Kingdom, 2018, pp. 965–973, <http://dx.doi.org/10.1145/3219819.3219822>.

Yan, J., Mu, L., Wang, L., Ranjan, R., & Zomaya, A. Y. (2020). Temporal Convolutional Networks for the Advance Prediction of ENSO. In *Scientific Reports* (Vol. 10, Issue 1). Springer Science and Business Media LLC. <https://doi.org/10.1038/s41598-020-65070-5>

Yang, Q., Lee, C.-Y., & Tippett, M. K. (2020). A Long Short-Term Memory Model for Global Rapid Intensification Prediction. In *Weather and Forecasting* (Vol. 35, Issue 4, pp. 1203–1220). American Meteorological Society. <https://doi.org/10.1175/waf-d-19-0199.1>

Yuan, S., Wang, C., Mu, B., Zhou, F., & Duan, W. (2021). Typhoon Intensity Forecasting Based on LSTM Using the Rolling Forecast Method. In *Algorithms* (Vol. 14, Issue 3, p. 83). MDPI AG. <https://doi.org/10.3390/a14030083>

Zhang, Z., Yang, X., Shi, L., Wang, B., Du, Z., Zhang, F., & Liu, R. (2022). A neural network framework for fine-grained tropical cyclone intensity prediction. In *Knowledge-Based Systems* (Vol. 241, p. 108195). Elsevier BV. <https://doi.org/10.1016/j.knosys.2022.108195>